NASA Contractor Report 165632

THERMAL EXPANSION PROPERTIES OF COMPOSITE MATERIALS

Robert R. Johnson, Murat H. Kural, and
George B. Mackey
Lockheed Missiles & Space Company, Inc.
Sunnyvale, California 94086

NASA

National Aeronautics and
Space Administration

Langley Research Center
Hampton, Virginia 23665

FOREWORD

This document was prepared by Lockheed Missiles & Space Company, Inc. (LMSC), P. O. Box 504, Sunnyvale, CA 94086, for the National Aeronautics and Space Administration – Langley Research Center, in compliance with Task Assignment No. 17, Contract NAS1-14887. This report is intended as a reference to the thermal expansion properties of various fiber-reinforced composite materials.

Harold G. Bush is the NASA Contracting Officer's Technical Representative on this program. The Program Manager and Project Leader at LMSC are H. Cohan and R. R. Johnson, respectively.

TABLE OF CONTENTS

LIST OF ILLUSTRATIONS

PRECEDING PAGE BLANK NOT FILMED

LIST OF ILLUSTRATIONS (Cont.)

TABLES

THERMAL EXPANSION PROPERTIES
OF COMPOSITE MATERIALS

Robert R. Johnson, Murat H. Kural, and George B. Mackey

SUMMARY

Thermal expansion data for several composite materials, including generic epoxy resins, various graphite, boron, and glass fibers, and unidirectional and woven fabric composites in an epoxy matrix, have been compiled into one comprehensive report.

A discussion of the design, material, environmental, and fabrication properties affecting thermal expansion behavior is presented. Test methods and their accuracy are discussed. Analytical approaches to predict laminate coefficients of thermal expansion (CTE) based on lamination theory and micromechanics are also included.

For space applications, a near-zero CTE is often highly desirable to maintain the thermal dimensional stability of a structure on-orbit. Although this is easily achievable with composite materials, it is often at the expense of some structural efficiency. A discussion is included of methods of tuning a laminate to obtain a near-zero CTE.

Related references that describe these data more extensively are included.

INTRODUCTION

It is well known that the high stiffness and low coefficient of thermal expansion (CTE) of graphite epoxy, together with its low density, make this material especially attractive for space applications.

Much data currently exist as the result of thermal expansion tests on graphite, Kevlar, boron, and glass fibers. Properties of composites, including unidirectional and woven fibers in epoxy, as well as some heat resins, are presented here. This document summarizes thermal expansion data obtained from published literature, as well as unpublished data from the LMSC data bank.

Factors that affect the thermal expansion properties are discussed briefly, and a related set of references that more extensively describe the influence of these factors is presented.

Use of commercial products or names of manufacturers in this report does not constitute official endorsement of such products or manufacturers, either expressed or implied, by the National Aeronautics and Space Administration

FACTORS AFFECTING THE CTE

The requirement of thermally stable space structures has led to the selection of fiber-resin composite materials to achieve a near-zero CTE. A number of factors affect the thermal dimensional stability of a laminate, and there is some question as to how close to zero CTE a laminate may be fabricated. Reference 1 presents the results of a rather thorough study of 29 test samples from one batch of pseudoisotropic GY70/X-30 material. Extension of the CTE data to a large sample indicated a 3 sigma statistical variation of close to $0.10 \times 10^{-6}/°F$ ($0.18 \times 10^{-6}/K$). Another analytical study (ref. 2), which includes material elastic constants, layup angle, material thickness, and input CTE data, indicates that for practical laminate designs, it is not feasible to specify a CTE less than $\pm 0.05 \times 10^{-6}/°F$ ($0.09 \times 10^{-6}/K$). This section contains discussions of the following factors

which affect the laminate CTE: fiber and void volumes, layup angle, fabric skewness, stacking sequence, thermal cycling, temperature dependence, moisture effects, and material viscoelasticity.

Fiber Volume

The dependence of CTE on fiber volume is illustrated in fig. 1 for a unidirectional layup. These curves were calculated based on formulas given in ref. 3. As seen in this figure, at approximately 60 percent fiber content, the longitudinal

(Ref. 3)
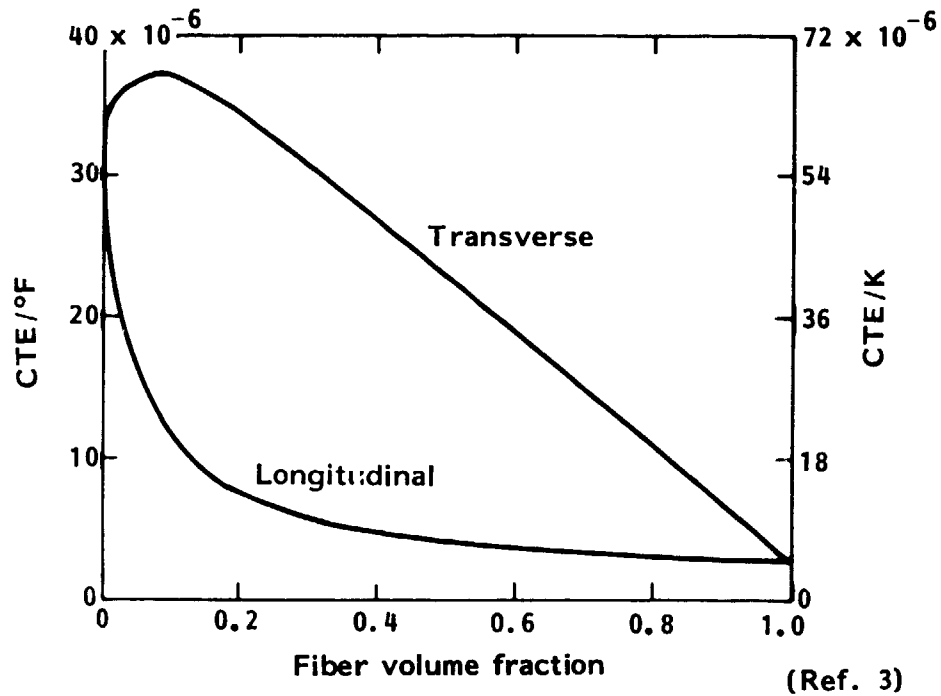
Figure 1. – Variation of CTE of a undirectional glass fiber laminate with fiber volume.

2

CTE is virtually unaffected by any changes in the laminate fiber content. In the case of transverse CTE, the sensitivity is more pronounced. In terms of angle ply laminates comprised of several layers, the effect of fiber volume variations on the thermal expansion behavior of the laminate may not be negligible.

Void Volume

The direct effect of voids on the CTE of composite laminates is small within the bounds of practical manufacturing requirements (1.5 percent max. void volume). However, the presence of voids can indirectly affect the CTE of a laminate by initiating microcracks in the resin. Voids in the resin also tend to increase the potential moisture content of the laminate. Both the microcrack and moisture effects are discussed in separate sections.

Layup Angle

One of the main advantages of laminated fiber reinforced composites is that mechanical and thermal response of the composites can be tailored directionally to satisfy design requirements. This is accomplished by varying the orientation of each layer in a systematic manner to reach the desired effect. Figure 2 shows the variation of CTE unidirectional and $\pm\theta$ angle laminates with fiber orientation (ref.4). The composite CTE can exceed the thermal expansion properties of single layers at certain angles for the $\pm\theta$ angle laminates. This phenomenon is predicted by laminate theory and also substantiated by tests.

The sensitivity of the composite CTE to variations from the intended fiber orientations can be severe. Although manufacturing tolerances for the layup angles are typically $\pm3°$, this practice can lead to serious CTE deviations for dimensionally critical structures. For example, a $5°$ deviation in the layup angle for the angle ply laminate shown in fig. 2 at approximately $\theta = 45°$ will cause almost an order of magnitude change in the value of the CTE of the laminate. Although this is an extreme case, it nevertheless points out the degree of sensitivity of certain classes of laminates to the change in the layup angle.

3
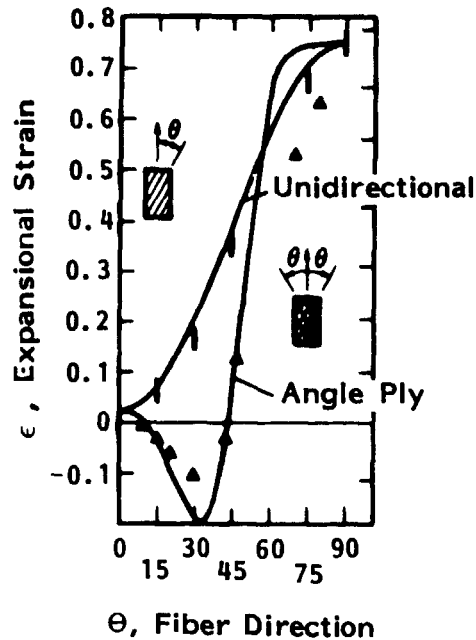
Figure 2. — Variation of expansional strain with laminate fiber orientation
(from ref. 4).

Fabric Skewness

Woven laminae have become quite popular for use with structural composites.
The effect of fabric skewness is to render the lamina monoclinic (one plane of sym-
metry). Thus, the lamina will display two axial coefficients and an independent
coefficient of thermal shear strain. Such laminae make it impossible to fabricate a
symmetric laminate. The behavior of unsymmetric laminates is well known. Woven
laminae should be handled with great care to avoid the inducement of fabric skew-
ness (e.g., avoid pulling a fabric on the bias).

Stacking Sequence

In general, if a laminate is symmetric and orthotropic (three mutually perpendic-
ular planes of elastic symmetry), the coefficients of free thermal strain are not a
function of stacking sequence. The presence of coupling response between bending

4

and extension behavior in an unsymmetric laminate will generally increase the co-efficients of thermal strain (expansion or contraction), because the effective laminate stiffnesses have been decreased. However, the laminate coefficients of thermal curvature are inversely proportional to laminate thickness and can be controlled by increasing the number of laminae within the laminate. For coupled laminates, the coefficients of thermal strain usually remain quite large compared to their symmetrical counterparts.

It is well known that if an unsymmetric laminate is restrained to closed geometry or zero curvature (e.g., cylindrical tubes or the unsymmetrical facings used to fabricate a symmetric laminate sandwich structure), the general response will appear as if the laminate was symmetric. However, for truly sensitive design applications involving CTEs, the reliability of this approach is questionable (ref.5).

For example, if a tubular member of $(0_3/+45)_T$ stacking sequence is fabricated to satisfy a particular design, the tube will not warp, bend, or bow as the closed geometry of the tube satisfies the symmetry condition. However, because in-plane symmetry conditions are not met in the wall, the tube will exhibit a thermal shear strain that will take the form of tubular twisting when exposed to thermal environments. If the tube is proposed to support an antenna, the deleterious effect of thermal shear strain is obvious. Thus, for sensitive thermal expansion designs, although unsymmetric laminates can be used, they must be used with great care.

Thermal Cycling

Thermal cycling is well known to have a significant effect upon the laminate CTEs. As shown in refs. 5, 6, and 7, the primary influence of thermal cycling is to induce resin microcracking. When microcracking occurs, and as it progresses, the laminate becomes partially decoupled, both thermally and mechanically. Resin degradation proceeds gradually at first, and then somewhat more rapidly, and can be detected by changes in the laminate thermal response. For single material laminates, the value of the laminate coefficient of expansion drifts toward the uni-directional CTE value of the material. This drift depends on many factors, including materials, rate and number of thermal cycles, temperature extremes, mechanical load level, and layup angle. For example, the drift of the CTE

5

of a cross-plied HMS laminate with $(0/90_2/0)_T$ layup cycled between -250°F and 250°F (116 K and 394 K) `as been observed to stop after nine cycles. Laminates with more gradual change ⅃ ᵢayer orientations usually take much longer to stabilize.

Temperature Depender e

It is a common practice to report the CTE of materials as a single quantity; these values are often used by designer. and analysts in the same manner. This practice may precipitate significant errors in composite design because of the temperature dependence of the thermal expansion behavior of composite materials. This temperature dependence is mainly caused by the mechanical and physical changes in the resin system. For this reason, the CTE values should be obtained from thermal expansion test data for the specific design temperature range. The CTE is a calculated value which is the slope of the thermal strain-temperature curve between two temperatures. This temperature dependence may be observed on many of the curves presented later in this document.

Moisture Effects

The dimensional stability ᴼf composites is highly affected by exposure to complex hygrothermal histories. Moisture causes swelling and plasticization of the resin system. The swelling phenomenon alters internal stresses, thus causing a dimensional change in the laminate. Coupled with plasticization of the resin system, ᵖ.rmanent dimensional changes of up to 30 percent have been observed in laboratory experiments after exposure to complex hygrothermal histories (ref.8). The importance of moisture on the thermal expansion behavior of graphite/epoxy composites is demonstrated in a study reported in ref. 9. The data shᴼwn in table I, extracted from the reference, demonstrate that dimensional changes caused by a temperature change of 118°F (339 K) are 2.09 $\mu\epsilon$, which is much less than the dimensional change due to moisture exposure (38.4 $\mu\epsilon$). It is therefore important to account for moisture effects in assessing dimensional changes due to thermal effects.

6

TABLE I. – CALCULATED STRAINS IN GY70/339 $[(0/90)_2]_s$ LAMINATE DURING HYGROTHERMAL CYCLING

Sequential hygrothermal history	Moisture content, percent water	ϵ_x $(\mu\epsilon)$
After cooling to 75°F (297 K) from 193°F (362 K) stress-free temperature	0.0	2.09
After exposure to 75°F (297 K)/95 percent RH for one year	0.65	38.4
After heating to 160°F (344 K) for 20 minutes	0.65	18.9
After desorbing at 125°F (325 K) for 128 days	0.0	7.22
After cooling to 75°F (297 K)	0.0	8.11

Viscoelasticity

As stated above, changes in the internal stresses due to moisture and thermal environment can result in significant dimensional changes in composite laminates. Internal stress levels also change due to the viscoelastic phenomenon called the relaxation of the resin system. In the true sense, relaxation of the internal stresses is a continuous process even without any mechanical, thermal, or moisture excursions. This process is usually minimized by placing fibers in the direction where dimensional stability is required. Graphite fibers are known to have negligible viscoelastic behavior.

PREDICTION OF CTE

The analytical methods used in the prediction of CTEs are presented in the following paragraphs. This review includes formulations based on lamination theory and the micromechanical approach. A more complete presentation of analytical methods discussed here can be obtained from the references listed later in this document.

Successful prediction of laminate thermal properties by the lamination theory is highly dependent on defining accurate mechanical and thermal properties of individual layers. In almost all cases, this is accomplished by testing unidirectional laminates. The micromechanical approach, where prediction is based on the

7

properties of constituent materials, is seldom used because of several factors. These factors include unavailability of constituent material properties, uncertainties in fiber data, and the inability of the micromechanical approach to define the transverse properties of the unidirectional laminate with high accuracy.

CTE by Lamination Theory

Classical lamination theory is based upon the concepts of linear anisotropic elasticity. Because of the stress and deformation hypotheses that are an inseparable part of classical lamination theory, a more correct name would be classical thin lamination theory, or even classical laminated plate theory. Strictly speaking, this theory is valid only for a solid homogeneous continuum, which is subjected to homogeneous boundary conditions. The approach and background for this analytical method are well developed in refs. 4, 7, and 10 through 12.

The general constitutive equation for a laminated plate is given by:

$$
\begin{bmatrix} \overline{N} + N^T \\ \hline \overline{M} + M^T \end{bmatrix}_i = \begin{bmatrix} A & B \\ \hline B & D \end{bmatrix}_{ij} \cdot \begin{bmatrix} \overline{\epsilon}^* \\ \hline \overline{K}^* \end{bmatrix}_j \quad (i,j = 1,2,6) \tag{1}
$$

This expression is used to relate the laminate mechanical stress resultants and stress couples, $\overline{N}_i$ and $\overline{M}_i$, to the laminate middle surface strains and curvatures, $\overline{\epsilon}_i^*$ and K_i^*. The laminate thermal stress resultants and stress couples are defined for a state of uniform (i.e., homogenous) temperature change:

$$
N_i^T = \Delta T \sum_{K=1}^{N} \overline{Q}_{ij}^K \, \overline{\alpha}_j^K \, [Z_K - Z_{K-1}] \quad \text{Thermal forces} \tag{2}
$$

$$
M_i^T = \frac{\Delta T}{2} \sum_{K=1}^{N} \overline{Q}_{ij}^K \, \overline{\alpha}_j^K \, [Z_K^2 - Z_{K-1}^2] \quad \text{Thermal moments} \tag{3}
$$

where,

$$
\Delta T = T_{OPERATE} - T_{REFERENCE}* \tag{4}
$$

---

*$T_{REFERENCE}$ is usually defined as the stress free temperature for the laminate.

8

The laminate stiffness matrices are also defined:

$$A_{ij} = \sum_{K=1}^{N} \bar{Q}^K_{ij} [Z_K - Z_{K-1}] \qquad \text{Extensional stiffnesses} \qquad (5)$$

$$B_{ij} = 1/2 \sum_{K=1}^{N} \bar{Q}^K_{ij} [Z^2_K - Z^2_{K-1}] \qquad \text{Coupling stiffnesses} \qquad (6)$$

$$D_{ij} = 1/3 \sum_{K=1}^{N} \bar{Q}^K_{ij} [Z^3_K - Z^3_{K-1}] \qquad \text{Bending stiffnesses} \qquad (7)$$

The geometric representation of a laminate is depicted in fig. 3. Both the laminate and lamina thicknesses (h and h_K) may be defined through the use of the following equation:

$$h = \sum_{K=1}^{N} h_K = \sum_{K=1}^{N} [Z_K - Z_{K-1}] \qquad (8)$$
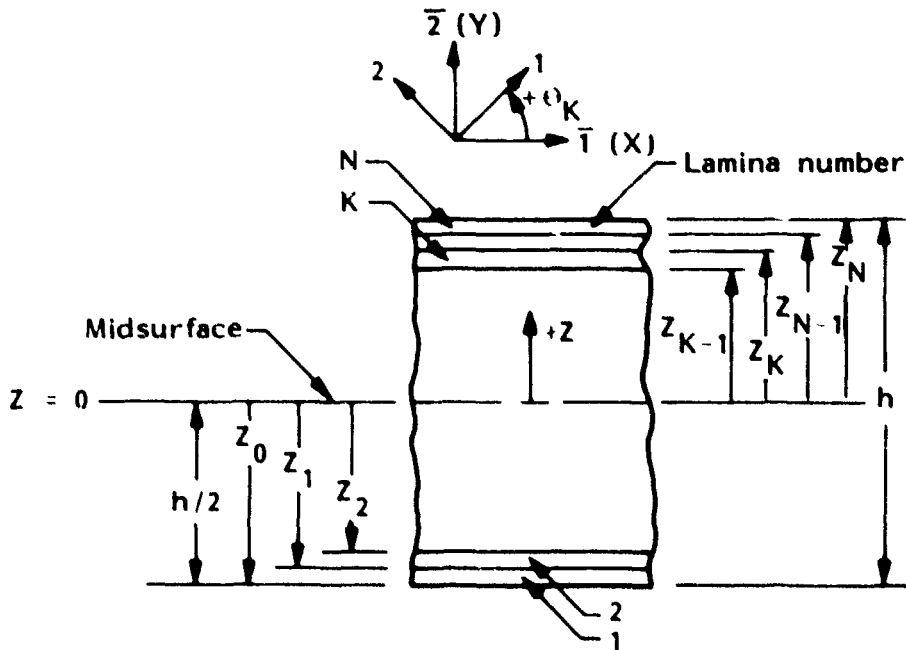
Figure 3. – Geometric representation of a laminate.

Note that $\bar{Q}^K_{ij}$ and $\bar{\alpha}^K_i$ are expressed in terms of the laminate coordinate system. The equations necessary to obtain the transformed lamina stiffnesses ($\bar{Q}^K_{ij}$) and transformed coefficients of free thermal strain ($\bar{\alpha}^K_i$) are given in table II. These transformations are linear and homogeneous. The invariant forms of the equations shown in table II were first given by Tsai and Pagano (ref. 13) in the

9

case of $\bar{Q}_{ij}^K$, and Halpin and Pagano (ref. 14) in the case of $\bar{\alpha}_i^K$. Note that the equations given in table II are sufficient to describe the transformation relationships for orthotropic laminae. This is a special, but highly practical, case.

TABLE II. – TRANSFORMATION EQUATIONS FOR $\bar{Q}_{ij}^K$ AND $\bar{\alpha}_i^K$
FOR THE Kth LAMINA

Term	Rotation invariant	$\cos 2\theta_K$	$\sin 2\theta_K$	$\cos 4\theta_K$	$\sin 4\theta_K$
$\bar{Q}_{11}^K$	U_1	U_2	O	U_3	O
$\bar{Q}_{22}^K$	U_1	$-U_2$	O	U_3	O
$\bar{Q}_{12}^K$	U_4	O	O	$-U_3$	O
$\bar{Q}_{66}^K$	U_5	O	O	$-U_3$	O
$\bar{Q}_{16}^K$	O	O	$1/2\ U_2$	O	U_3
$\bar{Q}_{26}^K$	O	O	$1/2\ U_2$	O	$-U_3$
$\bar{\alpha}_1^K$	W_1	W_2	O	O	O
$\bar{\alpha}_2^K$	W_1	$-W_2$	O	O	O
$\bar{\alpha}_6^K$	O	O	$2\ W_2$	O	O

where:

$U_1 = 1/8\ (3Q_{11} + 3Q_{22} + 2Q_{12} + 4Q_{66})$

$U_2 = 1/2\ (Q_{11} - Q_{22})$

For $\bar{Q}_{ij}^K$: $\quad U_3 = 1/8\ (Q_{11} + Q_{22} - 2Q_{12} - 4Q_{66})$

$U_4 = 1/8\ (Q_{11} + Q_{22} + 6Q_{12} - 4Q_{66})$

$U_5 = 1/8\ (Q_{11} + Q_{22} - 2Q_{12} + 4Q_{66})$

$r = E_{11}/(E_{11} - \nu_{12}^2\ E_{22})$

$Q_{11} = rE_{11}$

$Q_{22} = rE_{22}$

$Q_{12} = \nu_{12}\ Q_{22}$

$Q_{16} = Q_{26} = 0$

$Q_{66} = G_{12}$

For $\bar{\alpha}_i^K$: $\quad W_1 = 1/2\ (\alpha_1 + \alpha_2)$

$W_2 = 1/2\ (\alpha_1 - \alpha_2)$

10

To determine the laminate coefficients of free thermal strain (expansion, contraction, or shear) and free thermal curvature (bending or twisting), the mechanical stress resultants and stress couples must be equated to zero:

$$\overline{N}_i = \overline{M}_i = 0 \tag{9}$$

If equation (9) is now substituted into equation (1) and both sides of the resulting equation are divided by ΔT, the desired solution is obtained:

$$\frac{1}{\Delta T} \left[\begin{array}{c} N^T \\ \hline M^T \end{array} \right] = \left[\begin{array}{c|c} A & B \\ \hline B & D \end{array} \right]_{ij} \cdot \left[\begin{array}{c} \overline{\alpha}^* \\ \hline \overline{\lambda}^* \end{array} \right]_j \tag{10}$$

where:

$$\overline{\alpha}_i^* = \frac{\overline{\epsilon}_i}{\Delta T} \qquad \text{Laminate coefficients of free thermal strain} \tag{11}$$

$$\overline{\lambda}_i^* = \frac{\overline{K}_i^*}{\Delta T} \qquad \text{Laminate coefficients of free thermal curvature}$$

Equation (10) can now be used directly and solved by any algebraic method, including matrix inversion.

Lamina Micromechanics Formulation for CTE

There are two basic approaches to the micromechanics of composite materials (ref. 7):

(1) Mechanics of materials

(2) Elasticity.

The mechanics of materials approach embodies the usual concept of vastly simplifying assumptions regarding the hypothesized behavior of the mechanical system. The elasticity approach may include (1) bounding (variational) techniques, (2) exact solution, and (3) approximate solutions.

Irrespective of the micromechanical approach used, the usual restrictions on the composite material are:

Lamina	Reinforcement	Resin
Macroscopically homogenous	Homogeneous	Homogeneous
Linearly elastic	Linearly elastic	Linearly elastic
Macroscopically orthotropic	Isotropic	Isotropic
Initially stress-free	Regularly spaced	
	Perfectly aligned	

Although the expressions given in the literature for lamina CTEs vary, the results of Schapery (ref. 3) are widely quoted. The equation for the longitudinal CTE takes the form:

$$\alpha_1 = \frac{E_F \, \alpha_F \, \nu_F + E_m \, \alpha_m \, \nu_m}{E_F \, \nu_F + E_m \, \nu_m} \tag{12}$$

where:

$\quad E_F$ = Fiber modulus

$\quad E_m$ = Matrix modulus

$\quad \alpha_F$ = Fiber CTE

$\quad \alpha_m$ = Matrix CTE

$\quad \nu_F, \nu_m$ = Volume fractions

This equation is quite practical and is suitable for preliminary design. Similarly, the transverse CTE can be approximated by (ref. 3):

$$\alpha_2 = (1 + \nu_F) \alpha_F \, \nu_F + (1 + \nu_m) \alpha_m \, \nu_m - \alpha_1 (\nu_F \nu_F + \nu_m \nu_m) \tag{13}$$

However, care must be exercised in using this equation. It is at best an approximation.

References 15 through 20 contain additional information on micromechanical methods and CTEs.

THERMAL DIMENSIONAL STABILITY AND TUNING FOR ZERO CTE

This section discusses the thermal dimensional stability of laminated structures, including the tuning of laminates to obtain a near-zero CTE with a minimum effect upon structural efficiency.

Thermal Dimensional Stability

Factors affecting the CTE of a composite were discussed previously. Other factors include chemical and physical changes in the resin due to aging and solar/physical radiation. It is significant to note that even during a CTE test under laboratory conditions, the test specimen is not free from some of these effects, suggesting that the measured thermal strains in reality are the sum of strains caused by different effects.

Perhaps the most significant design criterion for composite structures requiring extreme dimensional stability is the determination of the specific mechanical and physical environmental spectrum the structure will go through during its lifetime. Once the environmental conditions are known, mechanical, physical, and thermal behavior of the composite structure can be determined using analytical and experimental techniques.

As the starting point, the designer selects the material and laminate configurations. Stiffness, strength, and CTE requirements determine the type of fibrous materials used in the structure. By determining the number of layers and properly orienting them, one can achieve a near-zero CTE laminate that will satisfy both the stiffness and strength requirements. Usually, there is more than one laminate configuration that will satisfy the preliminary requirements. For better thermal dimensional stability, the most likely laminate to succeed is the one that is least sensitive to changes affecting the CTE of the laminate.

A somewhat similar approach has been suggested and shown in refs. 21 and 22. A study was conducted on general $(O_i/\pm\theta)_s$ laminates to establish a configuration with a zero CTE that also satisfies the required mechanical properties. Results are shown in fig. 4.

Laminates with $(O/\pm\theta)_s$, $(O_2/\pm\theta)_s$, and $(O_3/\pm\theta)_s$ layups satisfy the zero CTE requirements for a specific θ. Also, the sensitivity of laminates to ply orientation

13

x 10⁻⁶ ... (figure)
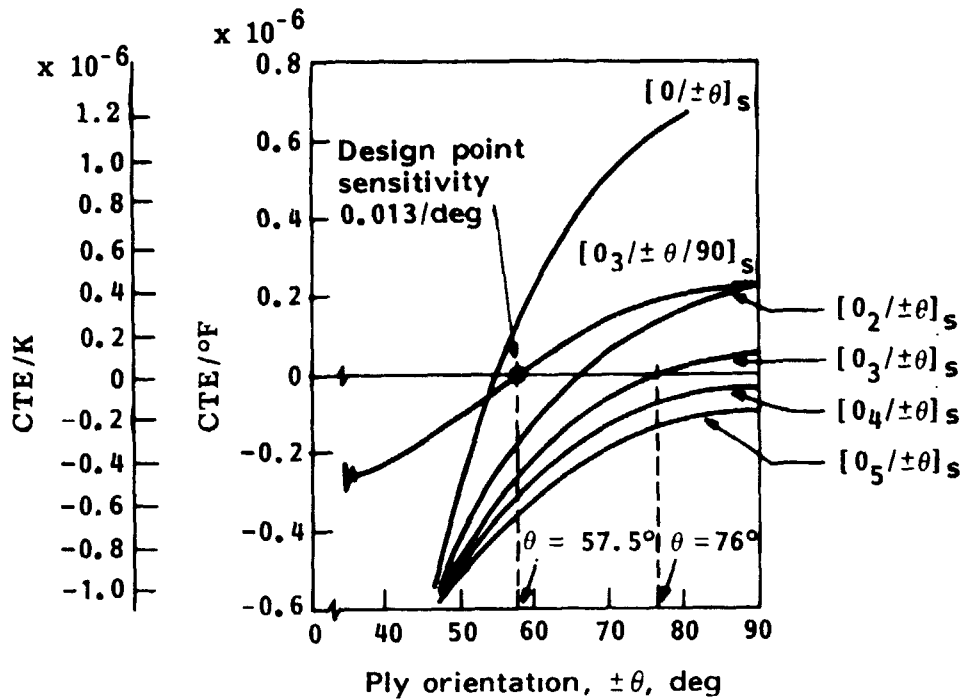
Figure 4. – Sensitivity of various laminates to layer orientation θ.

decreases with an increase in angle. For example, the slope of the expansion curve with the $(0_3/\pm\theta)_s$ layup is smaller than for the other two laminates mentioned above at zero CTE; thus, less sensitive to changes in angle θ. However, as angle θ gets larger, the shear stiffness of the laminate diminishes. To counteract this tendency, a 90° ply is added to the $(0_3/\pm76)_s$ laminate. The resulting laminate, $(0_3/\pm57.5/90)_s$, provides longitudinal extensional stiffness behavior nearly similar to the $(0_3/\pm76)_s$ laminate, but its shear stiffness is doubled. Results of computations for the two laminates are shown below:

Material and layups	α_x		E_x		G_{xy}	
	(x 10⁻⁶/°F)	(x 10⁻⁶/K)	Msi	(GPa)	Msi	(GPa)
HMS/934 $(0_3/\pm76)_s$	0.229	(0.41)	16.6	(112.8)	1.15	(7.8)
HMS/934 $(0_3/\pm57.5/90)_s$	0.229	(0.41)	14.4	(97.8)	2.31	(15.7)

Once a particular configuration is chosen, further sensitivity studies may be performed to establish the dimensional stability of the laminate as influenced by

14

other factors. A typical CTE sensitivity study is shown in table III. In each case, the baseline layer properties are increased 10 percent to obtain their effect on the composite CTE.

TABLE III. – $(0_3/\pm57.5/90)_s$ LAMINATE CTE SENSITIVITIES TO LAMINA PROPERTIES, BASELINE CTE = 0.41×10^{-6}/K (0.229×10^{-6}/°F)

Lamina properties	Change in laminate CTE	
	$(x\ 10^{-6}$/°F)	$(x\ 10^{-6}$/K)
E_{11}	$\dfrac{\partial\,(CTE)}{(10\%)E_{11}}$ = -0.056	-0.10
E_{22}	$\dfrac{\partial\,(CTE)}{(10\%)E_{22}}$ = +0.048	+0.09
G_{12}	$\dfrac{\partial\,(CTE)}{(10\%)G_{12}}$ = +0.001	0.002
α_1	$\dfrac{\partial\,(CTE)}{(10\%)\alpha_1}$ = +0.029	0.05
α_2	$\dfrac{\partial\,(CTE)}{(10\%)\alpha_2}$ = +0.052	0.09

Tuning Process

The tuning of a composite structure to obtain a near-zero CTE with a minimum effect on structural efficiency is not an easy task. Most conventional methods to drive or tune the CTE of the laminate to zero levels, such as changing the layups with different CTE characteristics, will usually result in a sacrifice of structural efficiency.

Theoretically, one of the most effective methods to achieve tuning without sacrificing the structural efficiency is to replace a percentage of the laminate fibers with an equally stiff but different CTE material. Results of a study showing the effect of adding boron, silicon carbide (SiC), FP (Al_2O_3), aluminum, or steel fibers to replace a percentage of graphite fibers in an epoxy laminate are shown in figs. 5 through 8. Specifically, laminates of VSB-32 pitch and GY70 fibers in an epoxy resin were examined. Results are shown in figs. 5 through 6 for unidirectional laminates and in figs. 7 and 8 for $(90/0/90)_T$ laminates. Material properties used in the analysis are given in table IV.

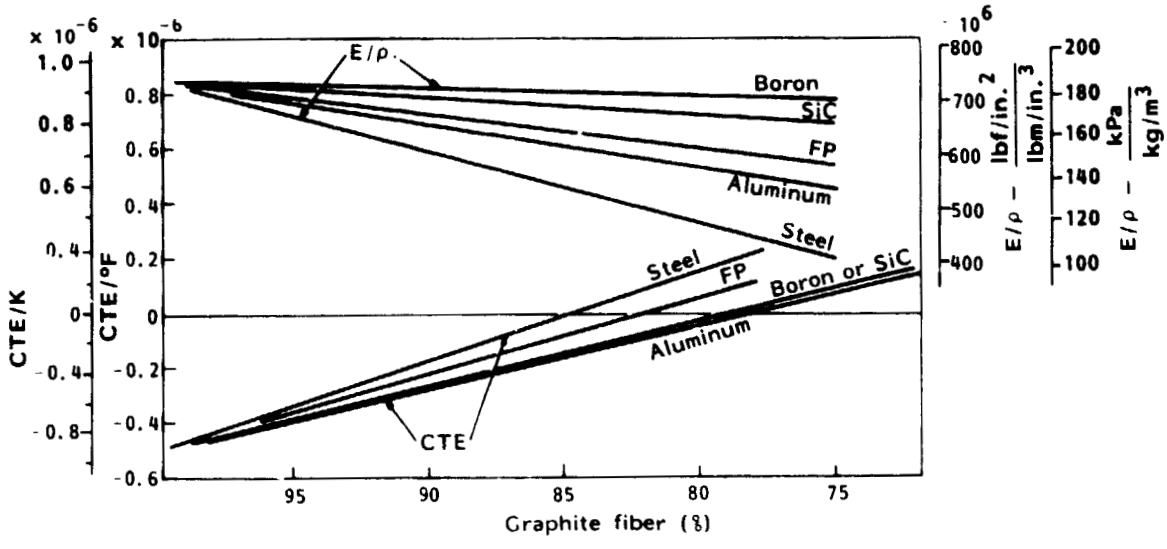Figure 5. – Effect of replacing GY70 fiber with other selected
fibers in a unidirectional laminate.
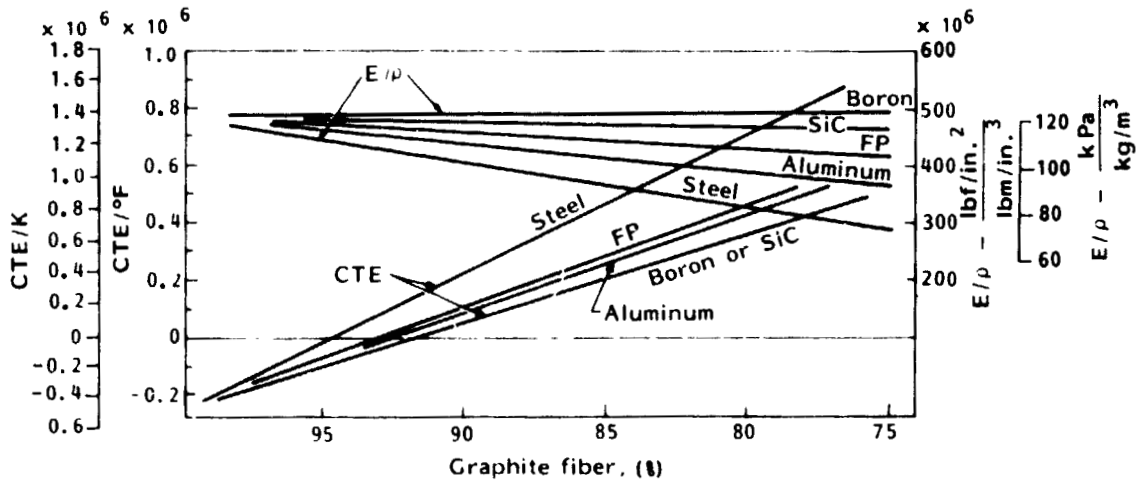
Figure 6. – Effect of replacing VSB-32 fiber with other selected
fibers in a unidirectional layup.

16
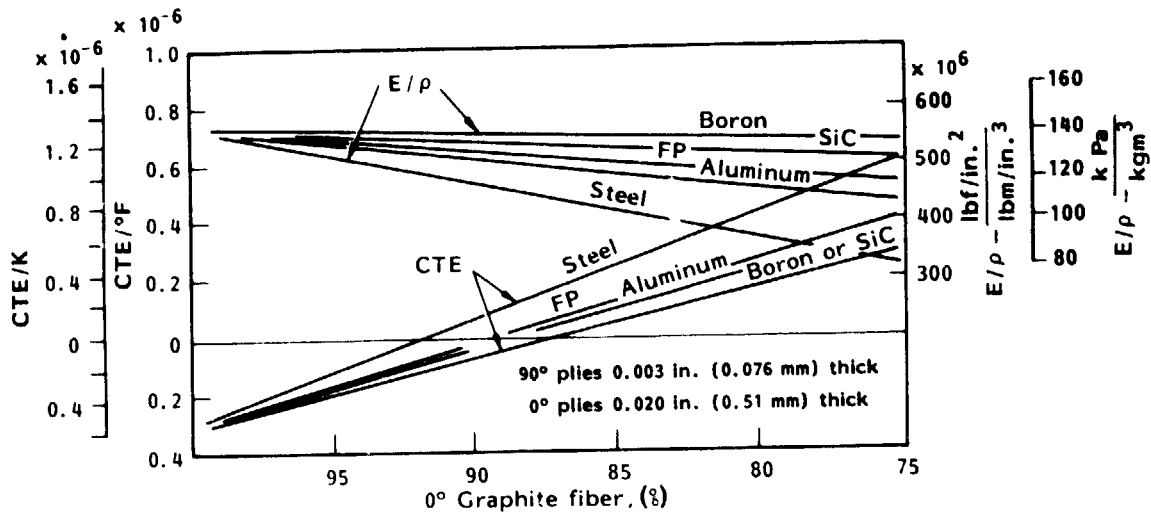
Figure 7. – Effect of replacing 0° GY70 fiber with other selected fibers in a (90/0/90) layup.
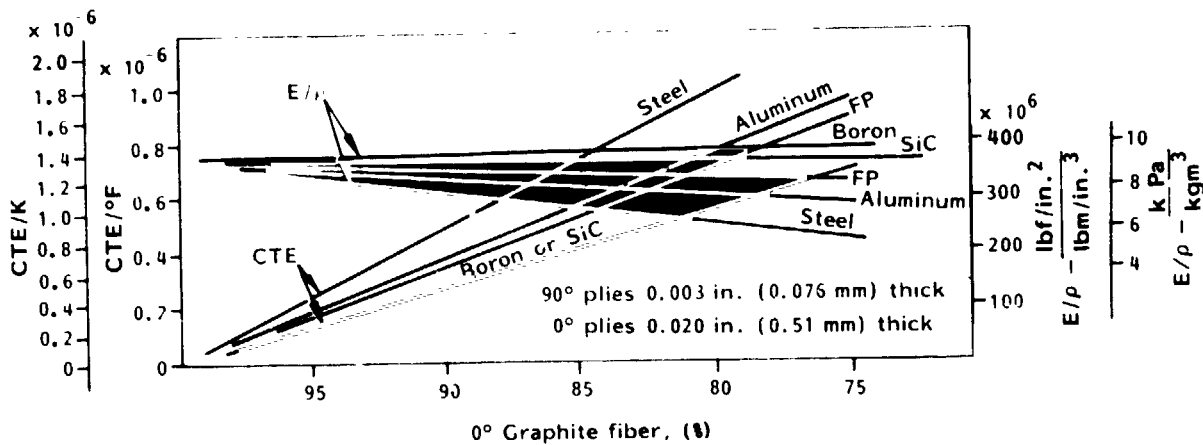
Figure 8. – Effect of replacing 0° VSB-32 fiber with other selected fibers in a (90/0/90) layup.

17

TABLE IV. – UNIDIRECTIONAL FIBER/EPOXY PROPERTIES – 60 PERCENT FIBER VOLUME

	CTE		Modulus of elasticity		Density		Merit function for CTE tuning (fiber only) $\frac{E\alpha}{\rho}$	
	(x 10^{-6}/°F)	(x 10^{-6}/K)	Msi	GPa	lb/in.^{3}	gm/cm^3	in./°F	m/K
GY70 Graphite	-0.50	-0.90	44	303.3	0.06	1.66		
VSB-32 Graphite	-0.25	-0.45	30	206.8	0.06	1.66		
Boron	2.40	4.32	34.8	239.9	0.072	2.00	1916	(87.60)
Silicon Carbide*	2.40	4.32	34.8	239.9	0.080	2.21	1526	(69.77)
FP (Al$_2$O$_3$)*	3.36	6.05	30.0	206.8	0.103	2.85	1123	(.34)
Steel*	7.30	13.14	17.4	120.0	0.187	5.18	720	(32.92)
Aluminum*	13.6	24.48	6.24	43.0	0.076	2.10	1329	(60.76)

*Rule of mixtures estimate

For GY70 (fig. 5), approximately 20 to 22 percent of the graphite must be replaced with boron, SiC, or FP to achieve a zero CTE. This is accomplished with almost no reduction in the specific modulus of elasticity for boron and about a 5 percent decrease for SiC.

Only about 7 or 8 percent of boron or SiC is required to obtain the zero CTE in unidirectional VSB-32 graphite epoxy (fig. 6). A very small decrease in specific stiffness is obtained as a result of using SiC, and a small increase in specific stiffness is achieved with boron fibers.

Steel and aluminum fibers were introduced for comparison purposes. When used to replace the VSB-32 fiber, 6 percent of the steel fiber is required as compared to 7 or 8 percent with boron or SiC. The decrease in specific modulus of elasticity is approximately 9 percent.

Similar results were obtained for a (90/0/90) laminate in which each of the 90° plies is 0.003 in. (0.076 mm) thick and the 0° or longitudinal ply is 0.020 in. (0.51 mm). For this portion of the study, a percentage of the 0° fibers was replaced by the hybrid fiber. These results are shown in figs. 7 and 8. In fig. 7, note that the replacement of about 12 or 13 percent of the GY70 fiber with SiC or boron will produce a zero CTE. The specific modulus of elasticity will decrease from 563×10^6 to $551 \times 10^6 \frac{\text{lbf/in.}^2}{\text{lbm/in.}^3}$ $\left(143 \text{ to } 140 \frac{\text{kPa}}{\text{kg/m}^3}\right)$ for the boron or SiC replacement.

For the VSB-32 fiber (fig. 8), the CTE of the (90/0/90) material is very close to zero. The addition of any replacement fibers will make the laminate CTE positive. It should be pointed out that the VSB-32 is still developmental. Any developmental increase in fiber modulus will make this (0/90/0) laminate negative; the addition of boron or SiC fibers will make the CTE of the laminate zero and also provide an increased stiffness.

An examination of the $\frac{E\alpha}{\rho}$ given in table IV indicates that an efficient procedure for tuning a laminate with a negative CTE is to select fibers with a high positive $E\alpha/\rho$ for partial replacement of the 0° fibers, and vice versa.

Novel Approaches to Tuning

Some rather innovative techniques have been developed by researchers to obtain near-zero CTE laminates, or structural configurations. A tunable end-fitting principle for struts is described in ref. 23.

Another novel approach to the tuning of composite struts is described in ref. 24. In particular, a "dual-alpha" concept is described in detail and a "variable-alpha" method is also briefly presented. The dual-alpha strut method is a relatively simple concept, which enables the attainment of a specific expansivity from parts whose as-cured CTE variability exceeds the design allowables. This method uses a laminated construction that exhibits expansivities along a strut length that are different from one another on either side of a transition zone length. In this manner, the expansion characteristics on either side of a transition zone bound the desired end-item expansivity. All final tuning (i.e., CTE adjustment) is then accomplished in the as-post-cured condition, thus accounting for most material and process variables (e.g., fiber volume). Tuning is accomplished using the as-cured material only. Additional parts or tuning "spacers," which are usually of a different material and therefore different thermal diffusivity, are not required. This then tends to enhance the thermal stability of the structure when subjected to transient thermal environments.

TEST METHODS

This section presents a brief discussion of the various test methods and techniques used to determine the composite CTE. The determination of CTE requires an approach that uses both length and temperature measurement techniques. The quality of the CTE data is directly dependent upon the accuracy and resolution potential of the equipment utilized. Since composite materials, as a class, may exhibit both very low and very high CTE values, it is often judicious to use combinations of test methods in the pursuit of a cost-conscious data-generation test plan. Wolff (ref. 25) provides an excellent and comprehensive discussion of composite CTE test techniques. Much of this discussion has been extracted from this reference.

Length Measurement Techniques

Table V (formulated from refs. 25 and 26) provides a summary of the general metrological groups and dimensional measurement techniques in accordance with their principles of operation. The accuracy of each method covers wide limits and

20

TABLE V. – SUMMARY OF TECHNIQUES FOR LENGTH MEASUREMENT

Measurement technique	Resolution, ϵ or (m)	Range, m or $\Delta\epsilon$ (%)	Accuracy, m or range (%)	Contact, no contact, or small gap, $<10\text{-}1$ (m)
A. Electrical transducers				
Resistance strain gages	10^{-7} (ϵ)	20%	5×10^{-7} (ϵ)	Contact
Semiconductor strain gages	10^{-9} (ϵ)	1%	10^{-8} (ϵ)	Contact
Capacitance	10^{-11}	10^{-4}	10^{-10}	Small gap
LVDT (dilatometers)	10^{-8}	10^{-2}	10^{-8}	Small gap
Electronic gages	10^{-9}	10^{-5}	10^{-9}	Contact
Resistance transducers	10^{-5}	3	1%	Contact
Variable impedence	10^{-8}	10^{-2}	0.01%	Small gap
Variable reluctance	10^{-6}	10^{-3}	3%	Contact
B. Electrical – optical transducers				
(1) Non-interferometric				
Autocollimator	3×10^{-6}	3%	10^{-5}	No contact
Fiber optics	10^{-8}	10^{2}	10^{-7}	Small gap
Optical levers	10^{-6}	10^{-1}	0.5%	No contact
Single beam shadowing	2×10^{-6}	10^{-2}	0.1%	No contact
Scanning beams	10^{-6}	10^{-2}	5×10^{-6}	No contact
Detector arrays	10^{-6}	$>10^{-1}$	10^{-5}	No contact
Photoelectric microscope	10^{-9}	10^{-4}	10^{-8}	Small gap
(2) Interferometric				
Michelson	$<10^{-9}$	10^{-3}	10^{-8}	No contact
Fabry – Perot	$<10^{-9}$	10^{-3}	10^{-8}	Contact
Fizeau	10^{-8}	10^{-3}	10^{-8}	Contact
Holographic	10^{-7}	10%	10^{-7}	No contact
Speckle	10^{-7}	~1%	10^{-7}	No contact
Moire	10^{-7}	~1%	10^{-7}	No contact

TABLE V. — Concluded

Measurement technique	Resolution, (m)	Range, m or $\Delta\epsilon$ (%)	Accuracy, m or range (%)	Contact, no contact, or small gap, $< 10-1$ (m)
C. Miscellaneous optical				
Diffraction pattern analysis	10^{-6}	$>10^{-5}$	$<10^{-7}$	No contact
Ellipsometry	10^{-10}	10^{-5}	10^{-10}	No contact
Spatial filtering	$\sim10^{-7}$	$>10^{-5}$	10^{-7}	No contact
D. Metrological				
Telemicroscopes	10^{-6}	1	10^{-6}	No contact
Dial gages	10^{-5}	10^{-2}	10^{-5}	Contact
Air gage	10^{-7}	10^{-3}	1%	Small gap
Micrometers	3×10^{-5}	10^{-1}	10^{-4}	Contact
Venier scales	3×10^{-5}	1	2×10^{-5}	Contact
Profile projectors	8×10^{-6}	1	10^{-5}	No contact
Micrometer slides	10^{-6}	10^{-1}	10^{-6}	Small gap

is, in general, a function of equipment modifications, accessories, and/or the ingenuity of the particular designer or user of the apparatus. Several methods suitable for linear displacement measurement on composite materials are described in the following paragraphs. Where possible, a primary consideration for a test technique is the elimination of contacts to the test sample or structure (e.g., see ref. 25 and table V).

Electrical Transducers for Displacement Measurement

Resistance strain gages are attached to the test sample by adhesive bonding. These gages are then used to determine the average strain ($\Delta L/L_o$) over a small area (i.e., gage area). Multiple gages can be employed to monitor displacements at multiple sites or in multiple directions, and to provide a temperature compensated circuit in a Wheatstone bridge unit. This approach is particularly useful for composite materials if sufficient care is taken to compare identical gage/adhesive sys-

22

tems on a reference material (e.g., fused silica, in the same bridge circuit). Potential problems with the use of these resistance strain gages include gage variability, local stiffening of thin sections, moisture, adhesive post cure effects, electrical heating, lead wires, and contact resistances. Further comments, including a brief discussion of semiconductor strain gages, can be obtained from refs. 25 and 27.

Capacitance methods, or capacity cell methods, can also be used to determine the composite CTE. The principles of operation involve the use of parallel plate condensers. The capacitance changes of these plates can be measured as the frequency changes of an LC oscillator circuit, where the plate spacing is proportional to the change in frequency. Calibration is required using identical sample materials on the capacitance cell/plate system. This technique is essentially a differential one, as described in ref. 25, requiring knowledge of the cell position (upper capacitance plate) during any run. Possible sources of error for capacity cell methods include edge capacitance effects, parallelism, sample sizes and shapes, and the time required to stabilize temperatures and record readings.

Linear Variable Differential Transformers (LVDTs) are used widely as a standard contact method for determining relative length changes. In practice, voltage is induced in the secondary winding of the transformer by the position of the axial core of the transducer. Commercial instruments (ref. 25) usually have a dc output proportional to the axial core position relative to the electrical center. Many dilatometers operate with LVDTs as the sensing element that is attached to a pushrod placed against an expanding sample in a furnace. Dilatometers using LVDTs are marginally useful for low CTE materials because of contacting errors, friction, alignment, and temperature effects on the LVDT itself. However, LVDTs have potentially infinite resolution, since the signal output is limited only by the ability to measure dc voltages, and the vibration stability of the core within the LVDT. Sources of error associated with the use of LVDTs and dilatometers, in addition to those mentioned above, include the power supply, recording instruments, and the standard (e.g., quartz) used to calibrate the LVDT-dilatometer system.

The majority of the LVDT-dilatometer test data given later in this report were obtained with the electrical (LVDT)-mechanical (quartz pushrod) system shown in fig. 9. The basic approach is described in ref. 26 (ASTM method of test 228-71).
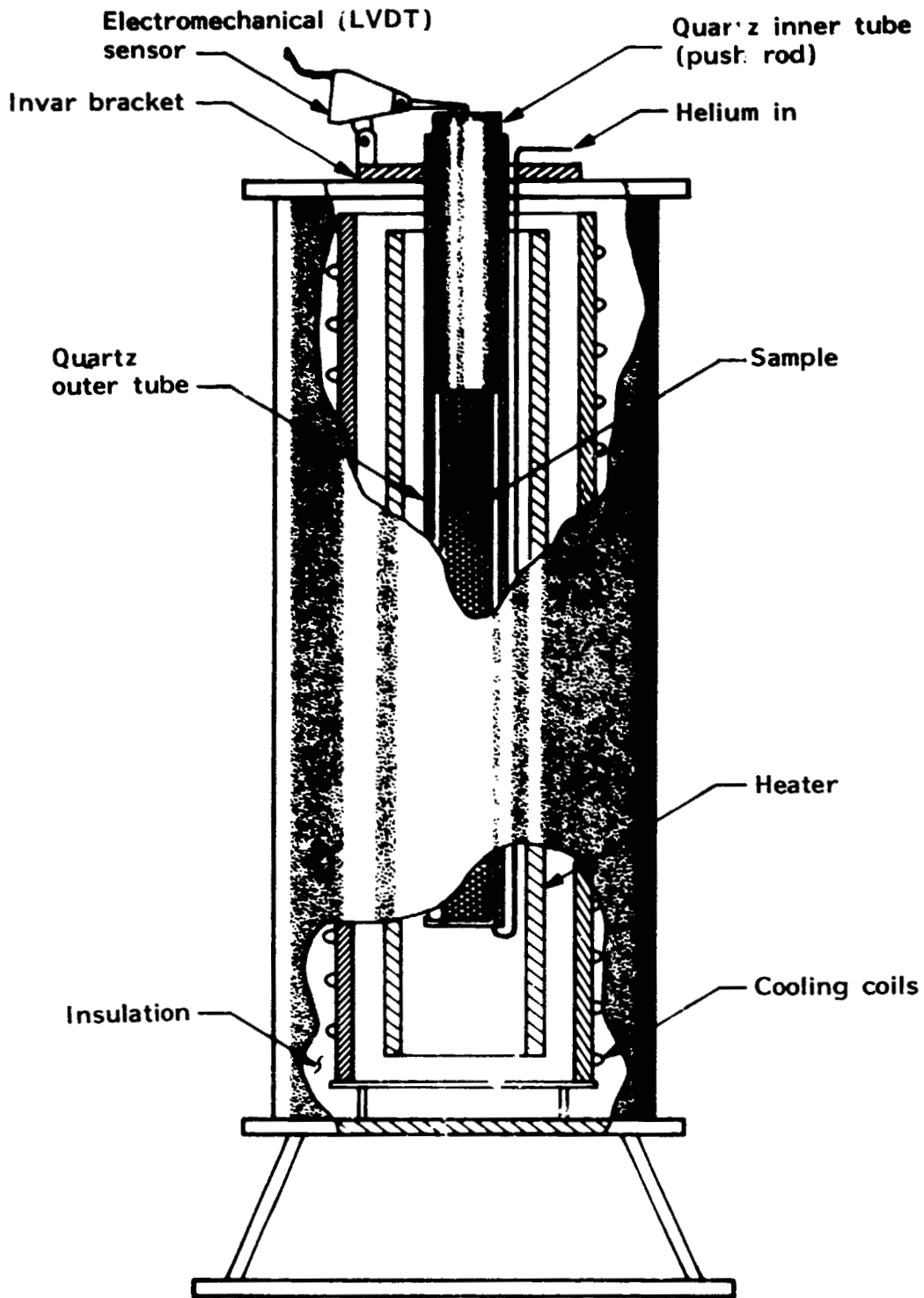
Figure 9. – Electromechanical dilatometer.

The apparatus shown in fig. 9 uses a specimen 12.00 ±0.010 in. long and 1-in. wide. Prior to measurements, the samples are preconditioned in the apparatus for 24 hours at 210 ±10°F (372 ±6K) with a dry helium purge. Each specimen is then subjected to two individual cycles during testing, since it is recognized that CTE tends to change with humidity and thermal history. The largest such changes usually occur during the first cycle.

Other dilatometric CTE methods used to generate the LVDT-dilatometer test data include the Netzsch dilatometer, modified Leitz dilatometer (fig. 10), and the dilatometer used in a thermomechanical analyzer (TMA).
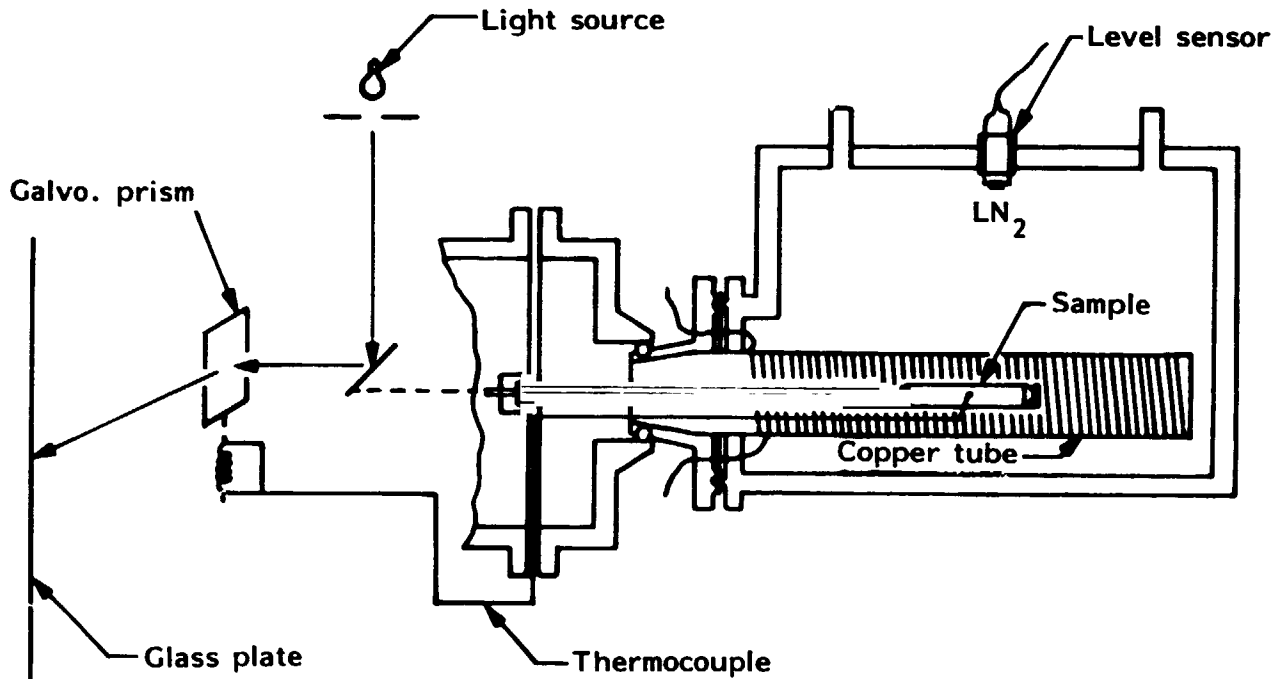

Figure 10. – Modified Leitz dilatometer.

The Netzsch dilatometer system basically consists of a fused silica stand and pushrod between which the test sample is inserted. The movement of the pushrod is transmitted to an iron core at the top of the rod that changes the inductance of

25

a transducer, thereby detuning a balanced ac bridge circuit, the rectified output of which is proportional to the specimen displacement.

The modified Leitz dilatometer system shown in fig. 10 is a mechanical-optical type method. This instrument is a typical quartz tube dilatometer in which the relative distance between ends is transmitted to the recording system by quartz rods that contact each end of the specimen. Relative movement of the quartz rods is transmitted to a rotatable prism by a mechanical lever system that magnifies the specimen displacement. A light beam projected through the prism passes through a lens system that further magnifies the displacement. Specimen size is restricted only by the size of the dilatometer. An unmodified pushrod type Leitz dilatometer is described in ref. 28.

The use, description, and explanation of the TMA method is well stated in ref. 29. This method is not recommended for measurements of low CTE materials, as the basic restrictions on specimen size alone may introduce a rather large percentage of error. Finally, electronic gages are often used for gage block comparators. These gages represent an extension of LVDT-type sensors with exceptional care taken to ensure accuracy and repeatability of readings.

Electrical-Optical Transducers for Displacement Measurement

Non-Interferometric Methods. — Auto collimaters use collimated light beams to detect small angular displacements of a reflecting surface area as small as 3×10^3 m in diameter. A sensitivity of 0.01 arc sec corresponds to a strain of $\sim 4.8 \times 10^{-8}$ m/m. This is achievable only with the use of electronic sensors. Visually, only strains of 10^{-5} can be detected (ref. 25). These instruments are suitable for monitoring the distortions of large structures for straightness or flatness.

Fiber optics bundles provide a noncontact method to provide optical measurements over distances of 10^{-2} m. The use of fiber optic methods can produce resolutions comparable to LVDTs (ref. 25). An advantage of this approach is that light beams can be diverted to reach otherwise inaccessible locations.

26

Interferometric Methods. – The interferometric method has been recommended by the ASTM (ref. 28). Its upper temperature of application is determined by the optical parts of the interferometer (e.g., 1,000 K for vitreous silica). The various interferometric methods are described in refs. 25, 28, 29, 30, and 31.

An interferometer recombines the two or more parts of a split light beam into a third beam whose intensity varies sinusoidally as the optical path length differences, relative to one (reference) beam, change by multiples of the wavelength (λ). The advent of the laser (laser interferometer) has provided the increased coherence needed to permit the widespread use of this approach for a variety of dimensional testing applications.

There are many types of interferometers, but thermal expansion measurements mainly employ the original Michelson interferometer (two-beam), and the Fabry-Perot and Fizeau interferometers (multiple reflections). It is fairly easy to count intensity variations, or fringes, as a sample expands or contracts when subjected to thermal excursions. This implies an immediate resolution potential of $\sim 10^{-6}$ m. For low expansion materials, however, fringe interpolation techniques are required. These include analysis of voltage outputs from photodiodes or photomultipliers, polarization and phase modulation techniques, and analysis of photographic plates (e.g., microdensitometry). Values of $\lambda/100 - \lambda/1000$ are presently the state of the art.

The Michelson interferometry method provides a measure of the relative displacement of the two reflecting surfaces. Figure 11 (extracted from ref. 25) represents a geometrical arrangement applicable to the study of hollow structures (e.g., tubes). Fabry-Perot interferometry methods require contact, but offer higher resolution potential than the Michelson approach. Fizeau interferometry (usually restricted to small samples) normally yields equal thickness circular fringes of very large radii of curvature (Newton's rings) depending on the contour of the reflecting surfaces.

Principal disadvantages of interferometric methods include the exposure of the measuring equipment to test environments, requirement of highly specialized, expensive equipment and difficulties, such as variation of air sources (e.g., changes in index of refraction), and target perturbations which can obliterate the time devoted to careful test setups.
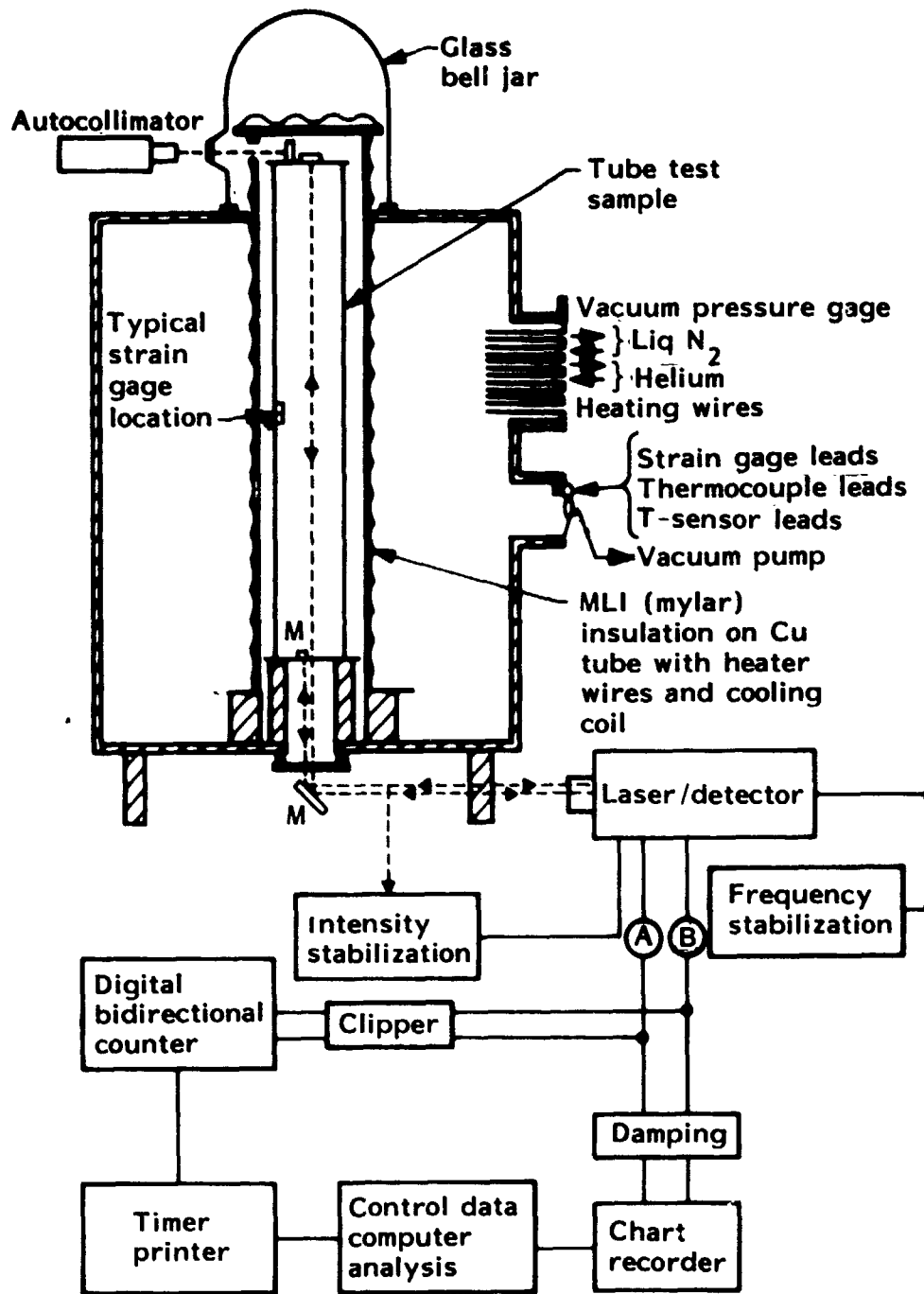
27

Figure 11. — Laser interferometer and dimensional stability
test apparatus.

Miscellaneous Op tical Methods for Displacement Measurement

Another important method is the diffraction pattern analysis which has been used to determine the CTE of E and S glass fibers. A laser beam illuminates the test object directly, resulting in a far-field diffraction pattern which is analyzed. When the diffracted light is collected with a lens, the pattern formed at its focal length is equivalent to the Fourier transform of the test object. Further comments can be found in ref. 25.

Other methods, described sufficiently elsewhere, are not covered here. (See refs. 25, 26, 28, 29, and 30.) In general, the telemicroscope method is directly applicable for CTE determinations of fibers, whereas, for example, dial gages (coupled with dilatometers as discussed in ASTM D-696, ref. 32) are suitable for the CTE determinations of resins, or very high CTE laminates.

THERMAL EXPANSION DATA

This section presents a summary of data relating to the CTE of fibrous composite materials. The CTE of reinforcements and some resin systems are included in addition to the fiber/epoxy data. The data presented were obtained as a result of a literature search, and these data have been supplemented with properties from the LMSC data bank. Fibers and resins that are no longer available were eliminated during the screening process.

The properties are presented in two formats. Tabular values of the CTE are listed for various temperatures as available from the literature. In addition, plots of free thermal strain (i.e., $\Delta L/L$) as a function of temperature are also presented as they are available. In some cases, the data have been replotted in an effort to achieve some consistency in the presentation. In other cases, the curves have been reproduced as they occurred in the original presentation.

Tables VI and VII list CTE values for various neat resin systems and fibers, respectively. Fiber materials include Kevlar-49, boron, graphite, and glass. Table VIII is a list of available composite thermal test data for unidirectional fibers and woven fabrics in epoxy matrix. Each table also includes test methods with which the CTE values have been obtained, and the origin of data (i.e., references).

TABLE VI. – COEFFICIENT OF THERMAL EXPANSION –
EPOXY RESIN SYSTEMS

Resin	Temperature		CTE		Test method	Source
	°F	K	x10⁻⁶/°F	x10⁻⁶/K		
Narmco 2387	RT 350	450	27 38	(48.6) (68.4)	LVDT Dilatometer	Ref. 33
3M PR 279	RT 350	450	25 70	(45) (126)	LVDT Dilatometer	Ref. 33
Ferro CE-3305	68-212	293-373	35.8	(64.4)	LVDT Dilatometer	Du Pont

Plots of free thermal strain as a function of temperature for various uni-directional and fabric composites are given in figs. 12 through 38. These plots are useful in determining the CTE of a lamina for a temperature range. that is not included in the tables. The value of the CTE is obtained by determining the slope of the curves between two temperatures.
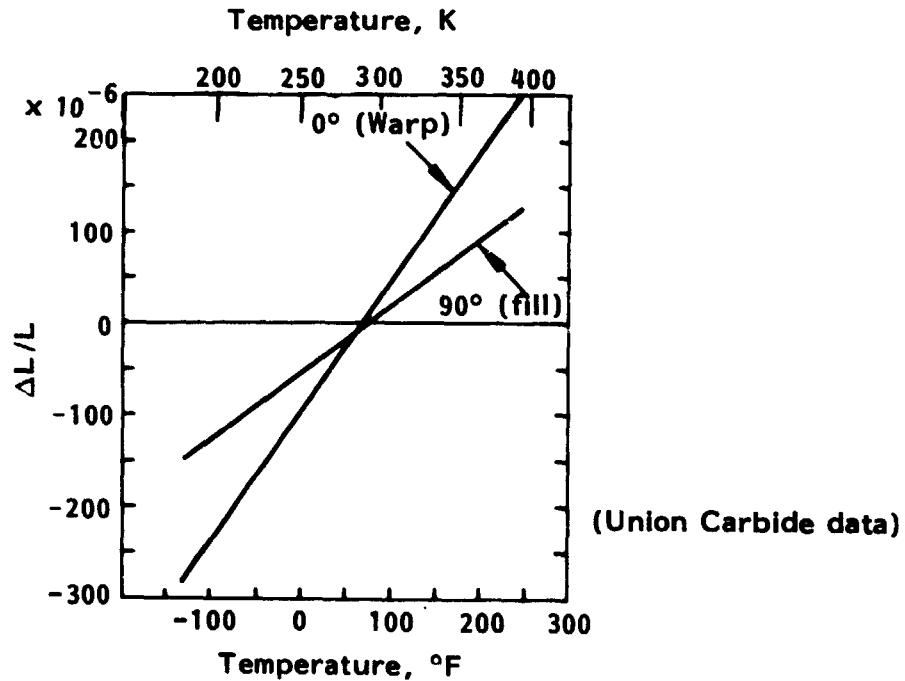

Figure 12. – Thermal expansion of Kevlar 49/X904B
(120 style) fabric.

30

TABLE VII. – COEFFICIENT OF THERMAL EXPANSION –
FIBROUS REINFORCEMENTS

Reinforcement	Temperature		CTE		Test Method	Source
	°F	K	x 10⁻⁶/°F	x 10⁻⁶/K		
Kevlar-49	32 to 212 212 to 392 392 to 500	273 to 373 373 to 473 473 to 533	-1.1 -2.2 -2.8	-1.98 -3.96 -5.04	Telemicroscope	Du Pont
Boron	RT		2.7	4.86	Unknown	Ref. 33
AS	RT		-0.23	-0.41	Telemicroscope	Hercules, Inc.
HTS	RT		-0.28	-0.50		
HMS	RT		-0.32	-0.58		
GY70	RT		-0.60	-1.08	Unknown	Celanese, Inc.
E-Glass	RT		2.8	5.04	Diffraction pattern	Ref. 34
S-Glass	RT		3.1	5.58	Diffraction pattern	Owens-Corning
S-2-Glass	RT		3.1	5.58		
Pitch (P75S)	-300 to +300°F	89 to 422	-0.7	-1.26	Unknown	Ref. 35
Pitch (95 msi)	RT		-0.85	-1.53	Unknown	Union Carbide
Pitch (50 msi)	RT		-0.28	-0.50		
Thornel 50 (PAN)	RT		-0.38	-0.68	Unknown	Ref. 36

31

TABLE VIII. – COEFFICIENT OF THERMAL EXPANSION – UNIDIRECTIONAL TAPE AND FABRIC EPOXY SYSTEMS

Material	Direction of test, degrees	Temperature		CTE		Test Method	Source
		°F	K	$\times 10^{-6}$/°F	$\times 10^{-6}$/K		
Kevlar/5134	0	-110 to 212	194 to 373	-1.28	-2.3	ASTM D696-44 (LVDT)	Du Pont
Kevlar/CE3305	0	-110 to 212	194 to 373	-2.22	-4.1		
Kevlar/E293	0	-319 to 248	78 to 393	-2.28	-4.1		
Kevlar/SP306	0	0 to 151	255 to 339	-1.94	-3.5		
Kevlar/CE3305	90	68 to 212	293 to 373	31.7	57		
Kevlar/E293	90	-319 to 248	78 to 393	19.4	35		
Kevlar/E293	90	194 to 347	363 to 448	32.2	58		
Kevlar/SP306	90	0 to 151	255 to 339	38.3	69		
Kevlar49/CE3305	0	68 to 212	293 to 373	0			
120 Style Fabric	90	68 to 212	233 to 373	0			
Kevlar49/X904B	0	RT		1.45	2.61	ASTM-E-228 (LVDT)	Ref. 36
120 Style Fabric	90	RT		0.7	1.3		
Kevlar49/5209	0	-65 to 160	219 to 344	2.8	5.0		
181 Style Fabric	90	-65 to 160	219 to 344	2.4	4.3		
Boron/AVCO5505	0	72	295	2.4	4.3	Modified Netzsch (LVDT)	Ref. 38
	0	100	311	2.4	4.3		
	0	200	366	2.5	4.5		
	0	300	422	2.8	5.0		
	0	350	450	3.0	5.4		
	90	72	295	12.3	22.1		
	90	100	311	13.5	24.3		

TABLE VIII. – CONTINUED

Material	Direction of test, degrees	Temperature		CTE		Test Method	Source
		°F	K	x10^{-6}/°F	x10^{-6}/K		
Boron/AVCO5505 Continued	90	200	366	18.6	33.5	Modified Netzsch (LVDT)	Ref. 38
	90	300	422	25.1	45.2		
	90	350	450	30.0	54.0		
AS/934	0	-100 to 100	200 to 311	0.075	0.14	Laser Interferometer	Ref. 22
	90	-100 to 100	200 to 311	14.3	25.7		
AS/828	0	-370 to -10	50 to 250	-0.28	-0.5	Capacity Cell	Ref. 39
	0	-10 to 260	250 to 400	1.22	2.2		
	90	-370 to -10	50 to 250	12.8	23.0		
	90	-10 to 260	250 to 400	28.7	51.7		
HTS/828	0	-370 to -10	50 to 250	-0.47	-0.85		
	0	-10 to 260	250 to 400	0.63	1.13		
	90	-370 to -10	50 to 250	11.1	20.0		
	90	-10 to 260	250 to 400	20.4	36.7		
HTS-2/3501-5A	0	-250 to -125	116 to 186	-0.19	-0.34	ASTM-E-228 (LVDT)	LMSC
	0	-125 to -25	186 to 241	-0.27	-0.49		
	0	-25 to 125	241 to 325	-0.22	-0.40		
	0	125 to 250	325 to 394	-0.08	-0.14		
	0	-250 to 0	116 to 255	-0.26	-0.47		
	0	0 to 250	255 to 394	-0.11	-0.20		
	0	-250 to 250	116 to 394	-0.19	-0.34		
	90	-250 to -125	116 to 186	9.00	16.2		
	90	-125 to 25	186 to 269	11.67	21.0		

TABLE VIII. - CONTINUED

Material	Direction of test, degrees	Temperature		CTE		Test Method	Source
		°F	K	x10⁻⁶/°F	x10⁻⁶/K		
HTS-2/3501-5A Continued	90	25 to 200	269 to 366	12.86	23.1	ASTM-E-228 (LVDT)	LMSC
	90	200 to 250	366 to 394	17.00	30.6		
	90	-250 to 0	116 to 255	10.10	18.2		
	90	0 to 250	255 to 394	13.80	24.8		
	90	-250 to 250	116 to 394	11.95	21.5		
Celion 6000/5213	0	73 to 180	296 to 355	-0.31	-0.56	Unknown	Celanese Corp.
	90	73 to 180	296 to 355	19.8	35.6		
Celion 3000/5213	0	173 to 350	351 to 450	-0.22	-0.40	Precision Dilatometer	Ref. 40
	90	173 to 350	351 to 450	15.0	27.0		
T-300/934	0	-303 to 75	89 to 297	0.05	0.09	Leitz Dilatometer	
	0	75 to 350	297 o 450	-0.04	-0.07		
	90	-300 to 75	89 to 297	11.3	20.3		
	90	75 to 350	297 to 450	18.7	33.7	(LVDT)	Ref. 37
T-300/5209	0	-65 to 160	219 to 344	0.05	0.09		
	90	-65 to 160	219 to 344	16.5	29.7		
T-300/PR313	0	-67	218	0.16	0.29	(LVCT)	Ref. 41
	0	72	295	0	0		
	0	260	406	0.13	0.23		
	0	350	450	0.13	0.23		
	90	-67	218	15.4	27.7		
	90	72	295	18.5	33.3		
	90	260	406	18.5	33.3		

34

TABLE VIII. – CONTINUED

	Direction of test, degrees	Temperature °F	Temperature K	CTE x10⁻⁶/°F	CTE x10⁻⁶/K	Test Method	Source
T-300/PR313 Continued	90	350	(450)	18.5	33.3	(LVDT)	Ref. 41
HMS/3051-5A	0	-250 to -150	116 to 172	-0.30	-0.54		
	0	-150 to -50	172 to 227	-0.38	-0.68		
	0	-50 to 50	227 to 283	-0.33	-0.59		
	0	50 to 150	283 to 339	-0.22	-0.40		
	0	150 to 200	339 to 366	-0.18	-0.32		
	0	200 to 250	366 to 394	-0.18	-0.32		
HMS/3501-5A	90	-250 to -150	116 to 172	9.50	17.1		LMSC
	90	-150 to -50	172 to 227	11.00	19.8	ASTM-E-228	
	90	-50 to 50	227 to 283	12.50	22.5	(LVDT)	
	90	50 to 150	283 to 339	13.75	24.75		
	90	150 to 200	339 to 366	14.50	26.1		
	90	200 to 250	366 to 394	17.00	30.6		
T-50(PAN)	0	-250 to -150	116 to 172	-0.29	-0.52		
	0	-150 to -50	172 to 227	-0.41	-0.74		
	0	-50 to 50	227 to 283	-0.39	-0.70		
	0	50 tc 150	283 to 339	-0.34	-0.61		
	0	150 to 250	339 to 394	-0.27	-0.49		
	0	-250 to 250	116 to 394	-0.34	-0.61		
GY70/X-30	0	-300 to 250	89 to 394	-0.48	-0.86	'ecision Dilatometer Modified Lietz (LVDT)	} Ref. 40
	90	-300 to 250	89 to 394	15.50	27.9		

35

TABLE VIII. – CONCLUDED

Material	Direction of test, degrees	Temperature		CTE		Test method	Source
		°F	K	$\times 10^{-6}/°F$	$\times 10^{-6}$ K		
P75S/934	0	-300 to 300	89 to 422	-0.57	-1.03	Unknown	Ref. 35
	90	-300 to 300	89 to 422	14.2	25.5		
Chopped fiber for molding compound	0	RT		0.19	0.34	Unknown	Ref. 42
E-Glass/epoxy	0	RT		3.5	6.3	Unknown	Ref. 41
	90	RT		11.4	20.5		
Glass/F163 7781 style fabric	0	RT		4.79	8.6	Unknown	Hexcel Corp.
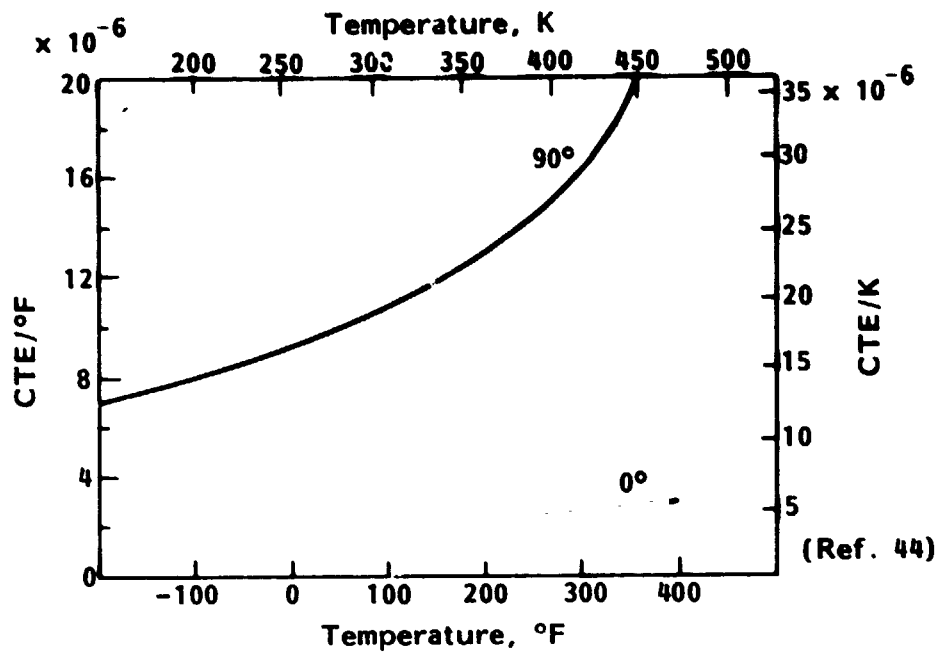
Figure 13. – Thermal expansion of unidirectional Boron/5505 tape.
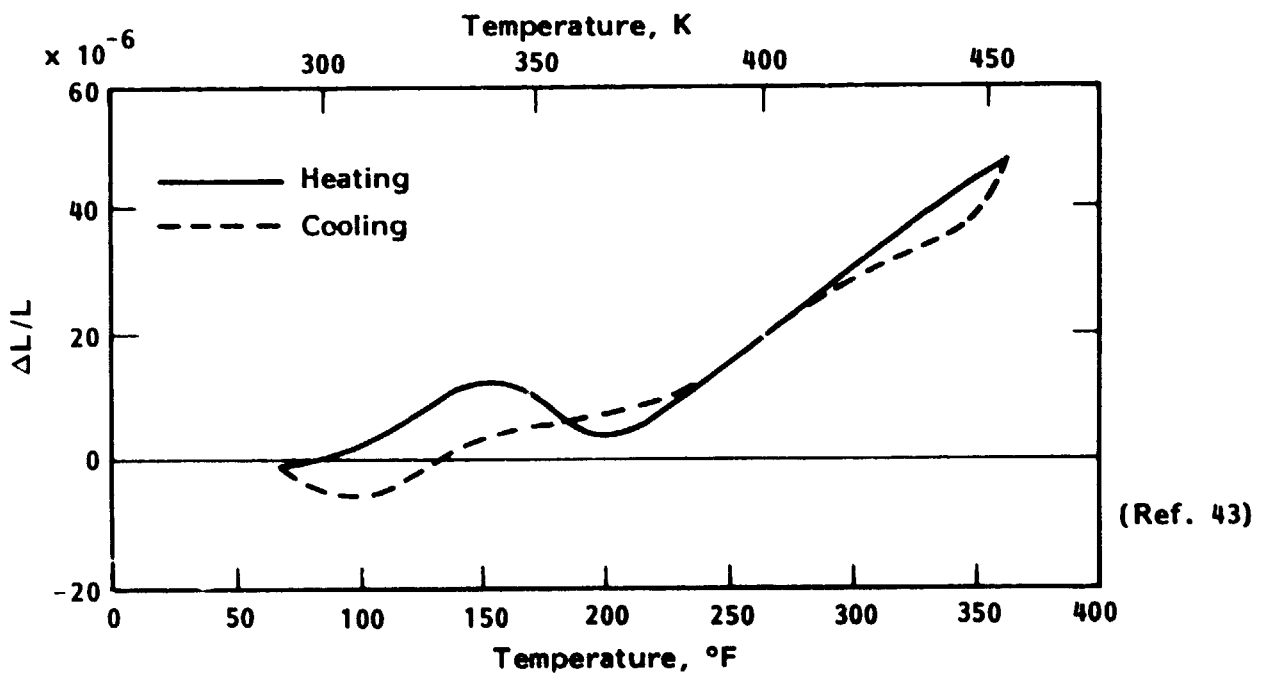
Figure 14. – Thermal expansion of Thornel 300/Narmco
5208 tape (0° fiber direction).
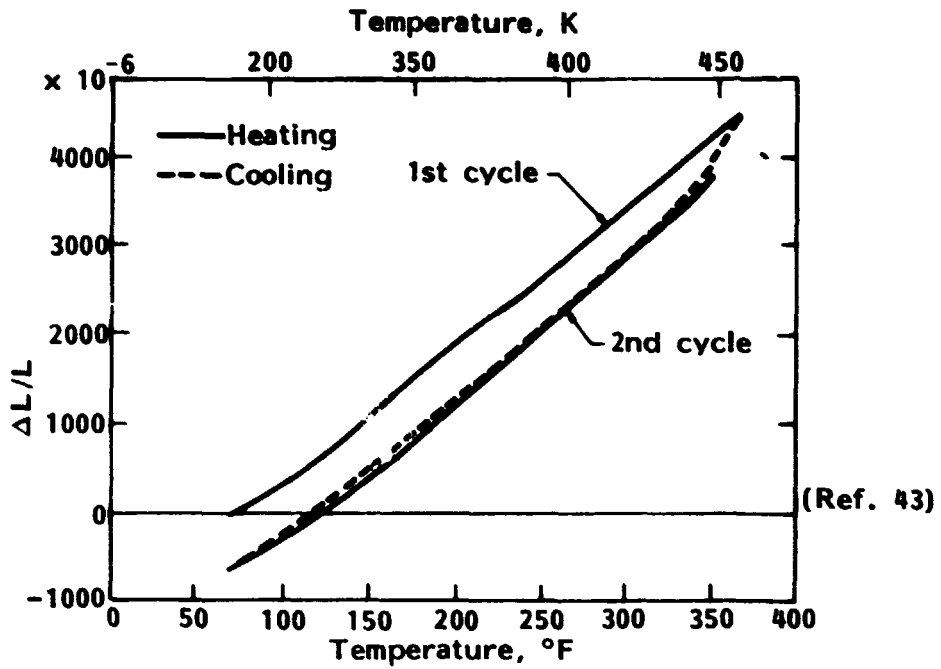
Figure 15. — Thermal expansion of Thornel 300/Narmco
5208 tape (90° fill direction).
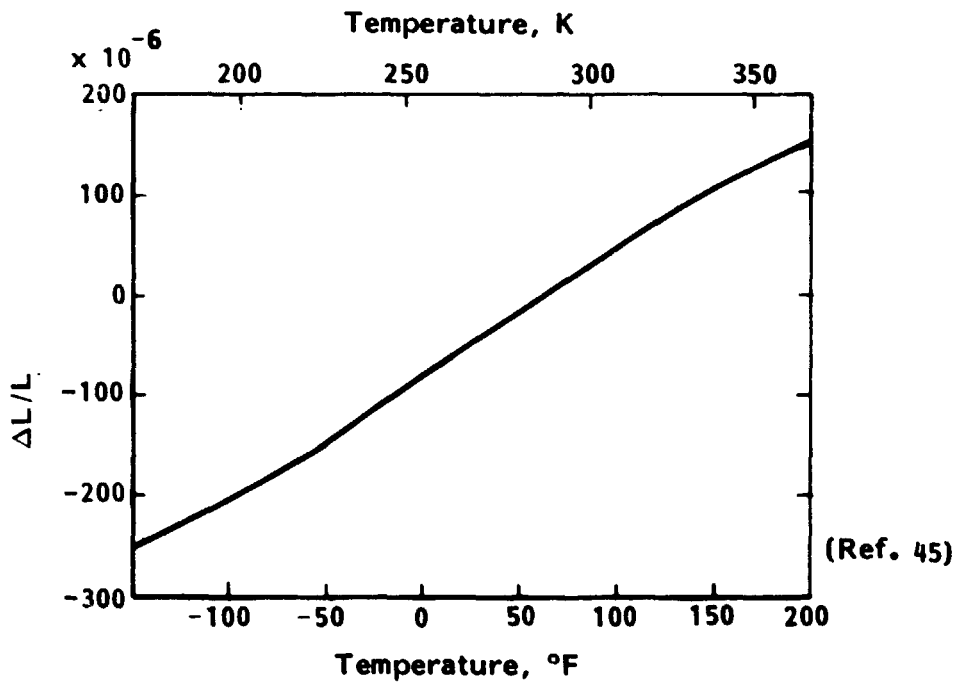
Figure 16. — Thermal expansion of HMF 330C/CE339 fabric
(T-300 fiber) (0° warp direction).

38
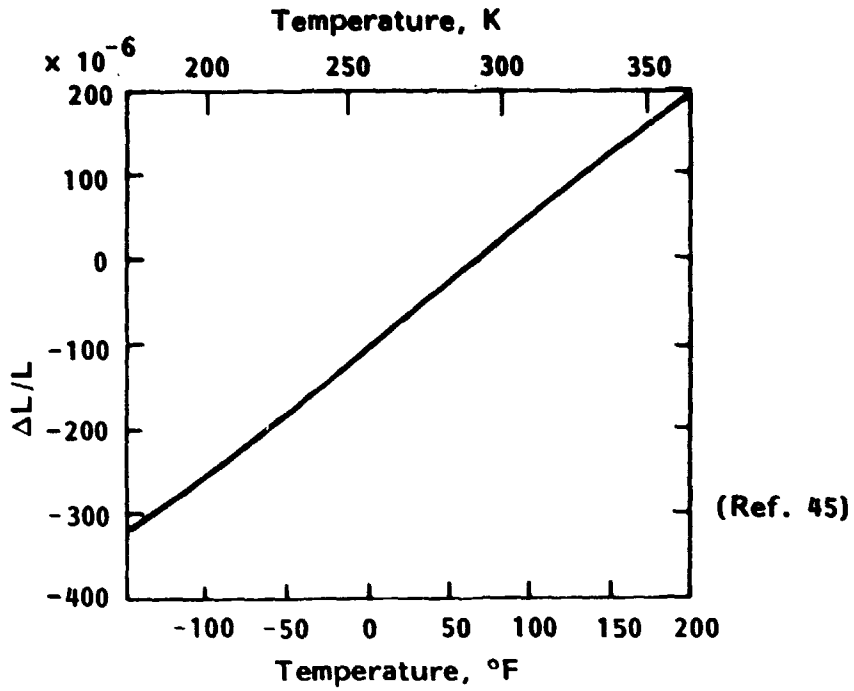
Figure 17. – Thermal expansion of HMF 330C/CE339 fabric
(T-300 fiber) (90° fill direction).
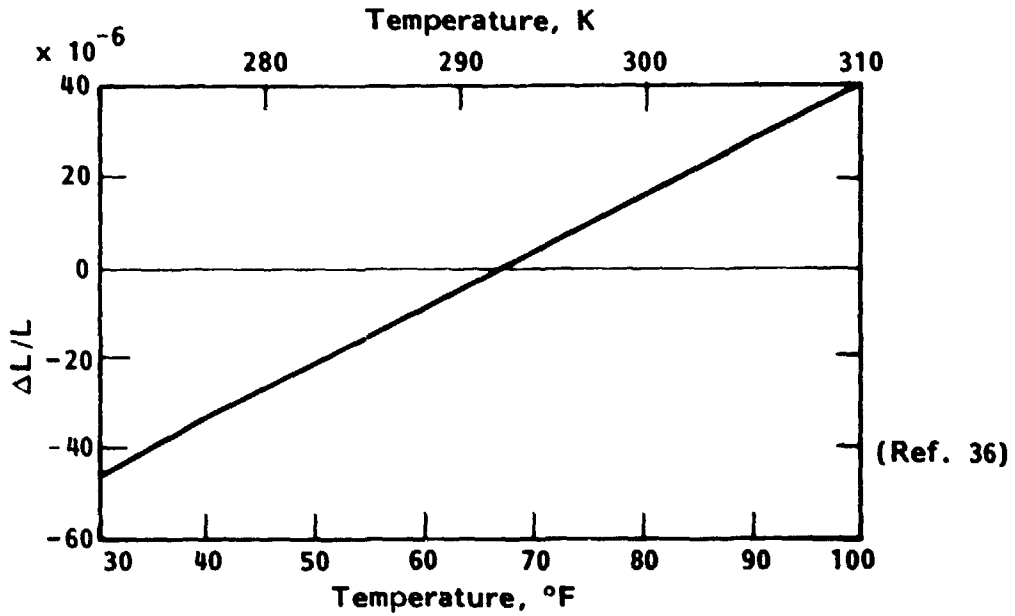
Figure 18. – Thermal expansion of HMF 330C/934 fabric
(T-300 fiber) (0° warp direction).

39
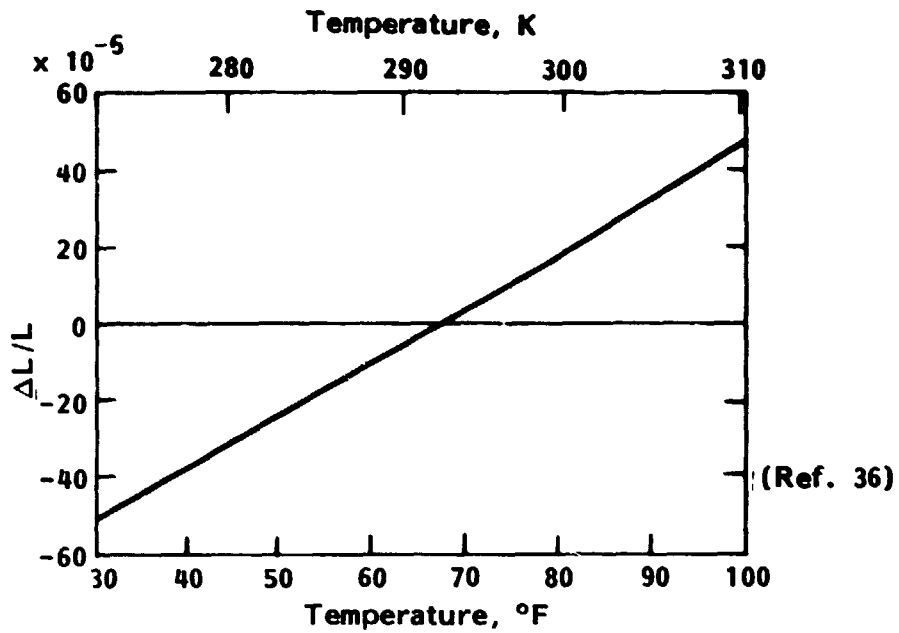
Figure 19. – Thermal expansion of HMF 330C/934 fabric
(T-300 fiber) (90° fill direction).
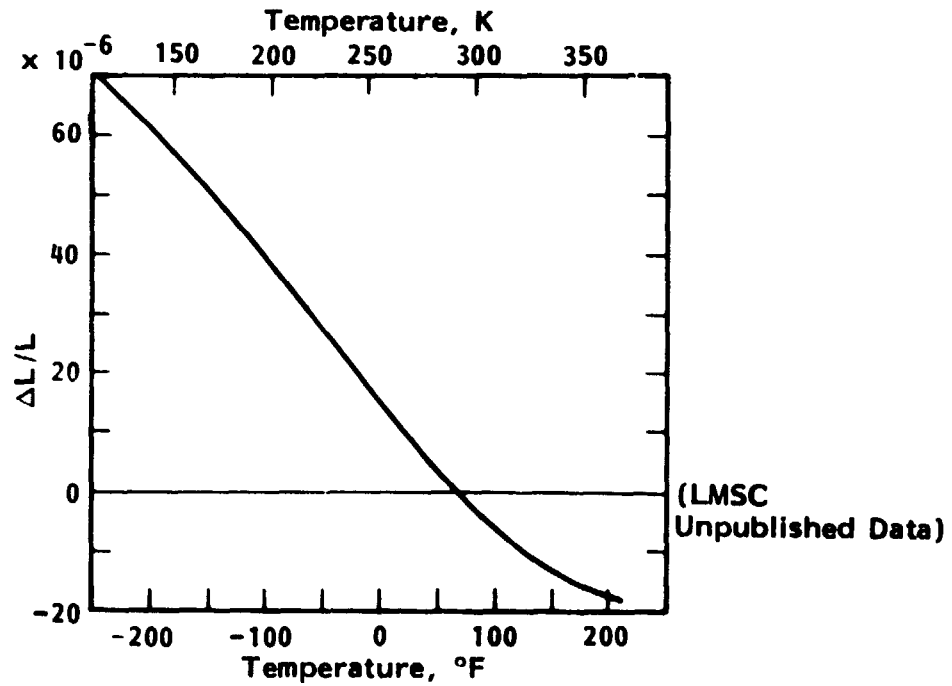
Figure 20. – Thermal expansion of unidirectional
HTS-2/3501-5A tape (0° fiber direction).

40
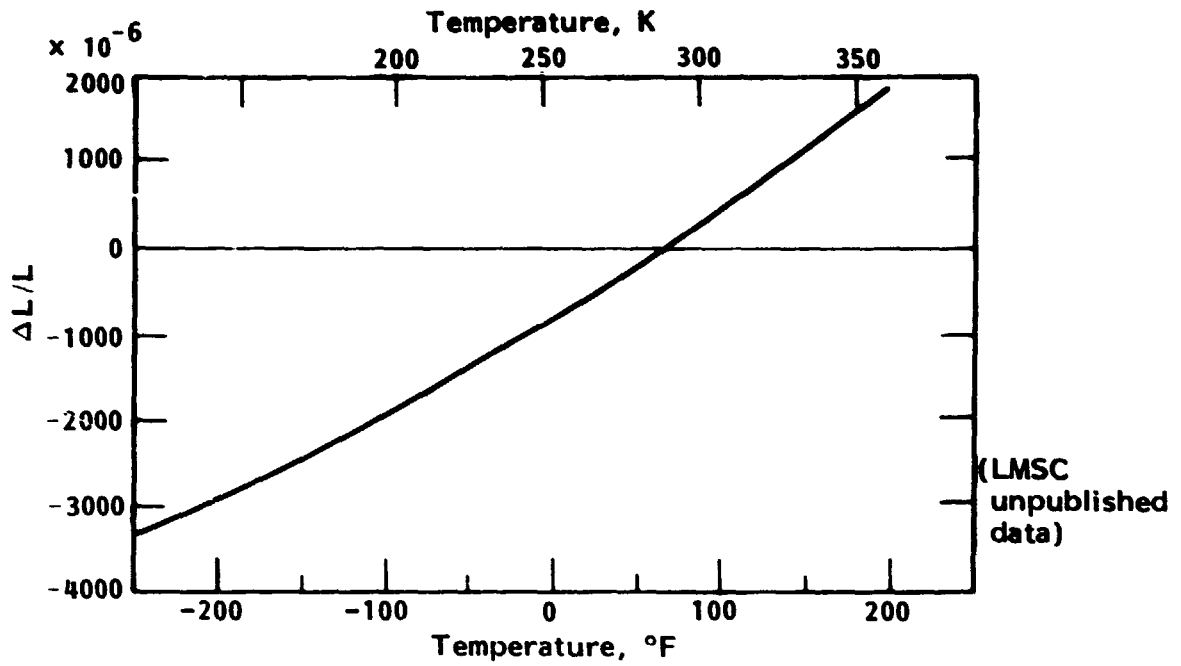
Figure 21. – Thermal expansion of unidirectional HTS-2/3501-5A
tape (90° fiber direction).
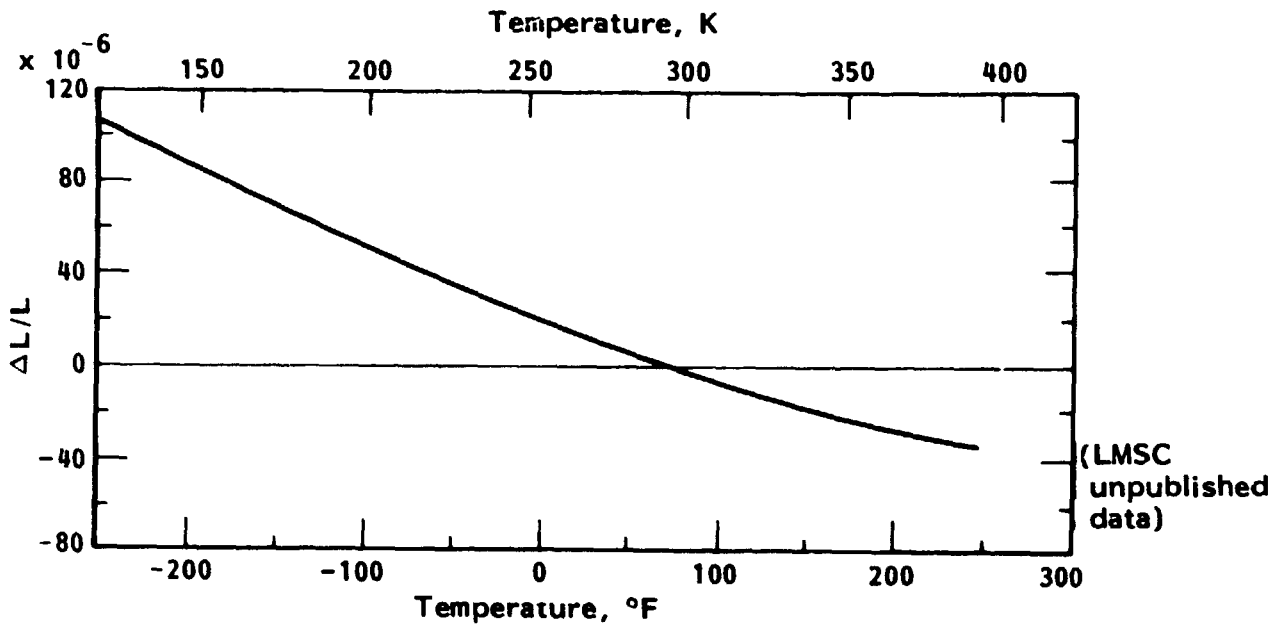
Figure 22. – Thermal expansion of unidirectional HMS/3501-5A
tape (0° fiber direction).

41
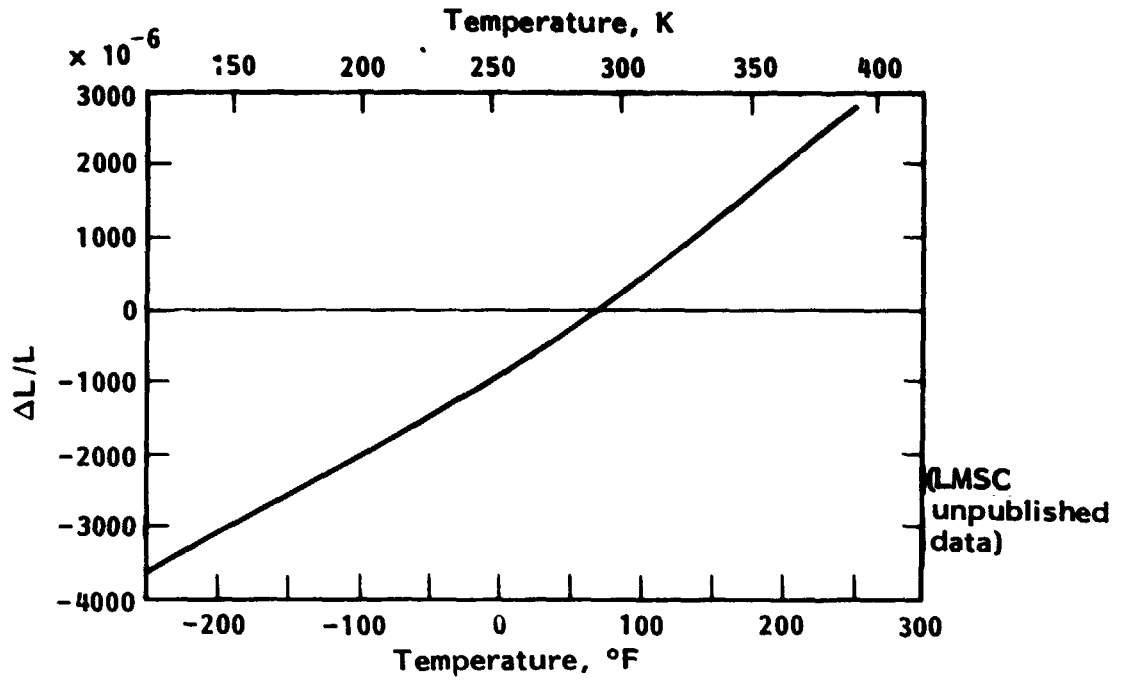
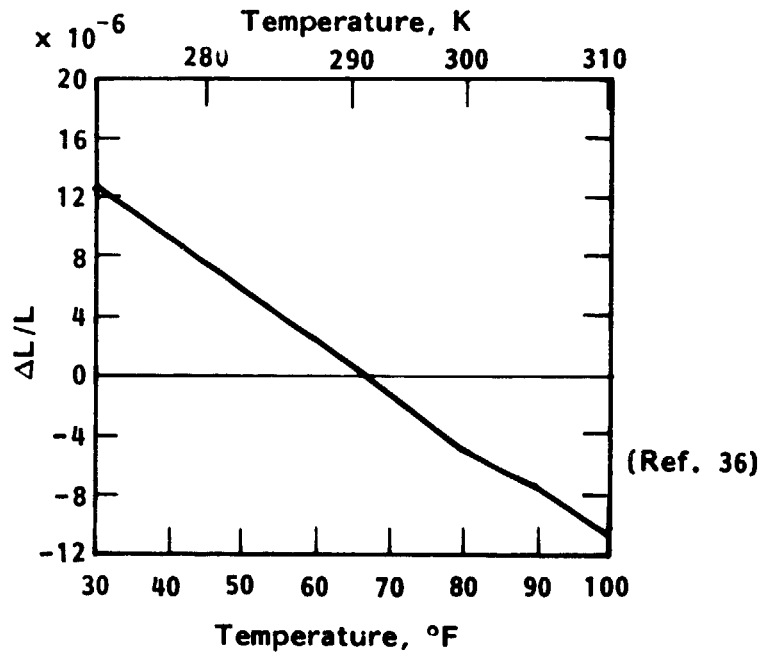Figure 23. – Thermal expansion of unidirectional HMS/3501-5A tape (90° fiber direction).
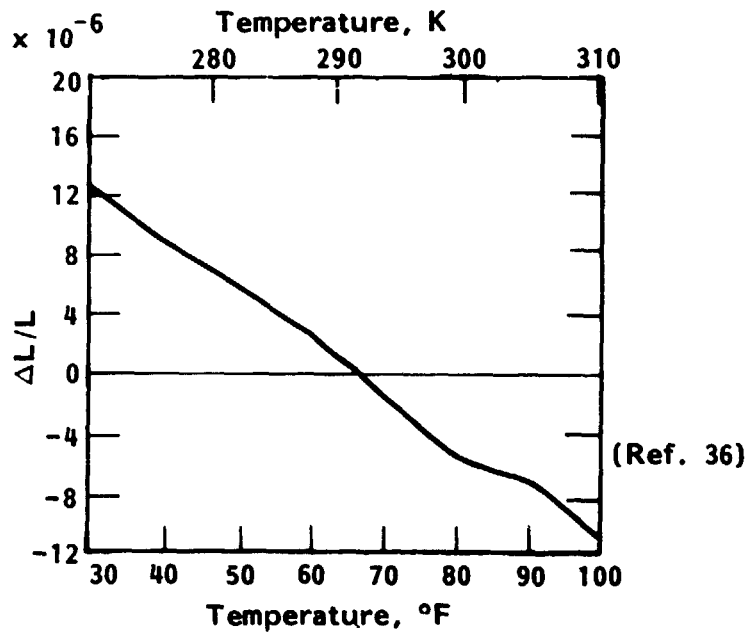
Figure 24. – Thermal expansion of HMS/3501 unidirectional tape (0° direction).

42
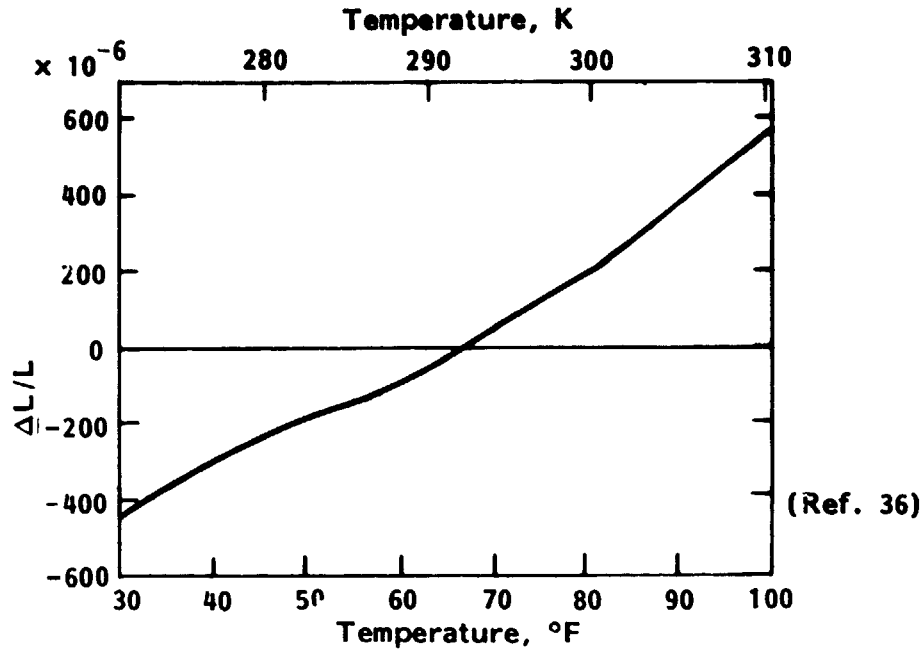
Figure 25. – Thermal expansion of HMS/3501 unidirectional
tape (90° direction).
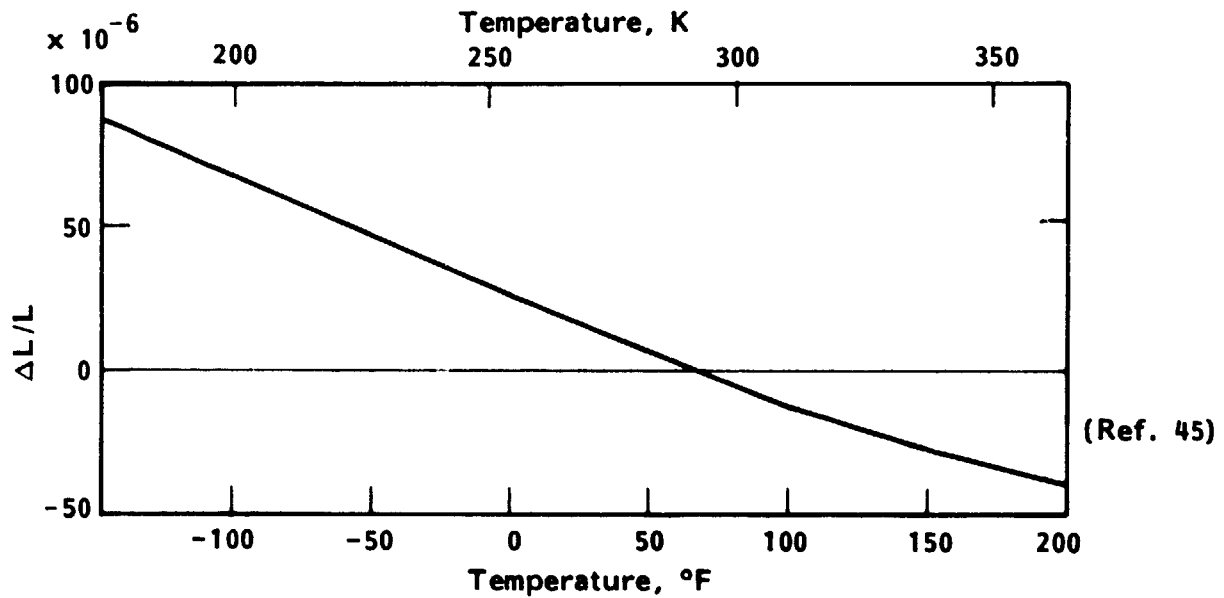
Figure 26. – Thermal expansion of HMS/CE339
unidirectional tape (0° fiber direction).
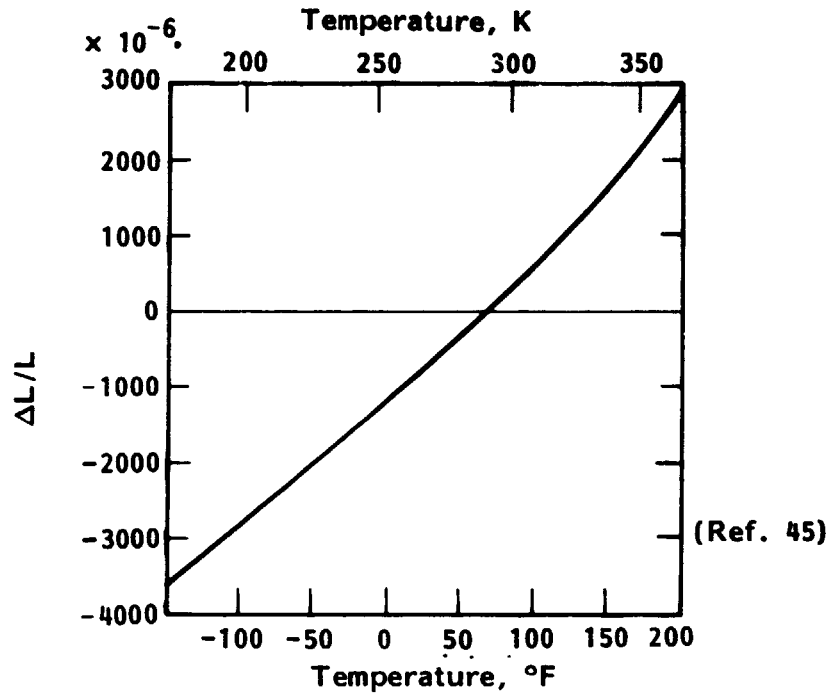
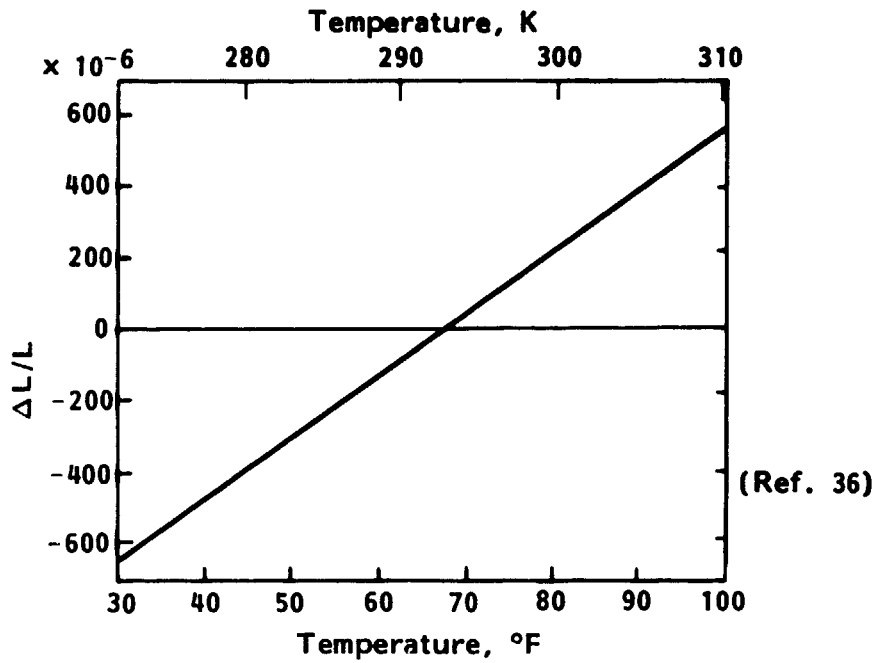Figure 27. – Thermal expansion of HMS/CE339 unidirectional tape (90° fiber direction).

Figure 28. – Thermal expansion of HMS/759 unidirectional tape (0° direction).

44

Figure 29. – Thermal expansion of HMS/759 unidirectional tape (90° direction).
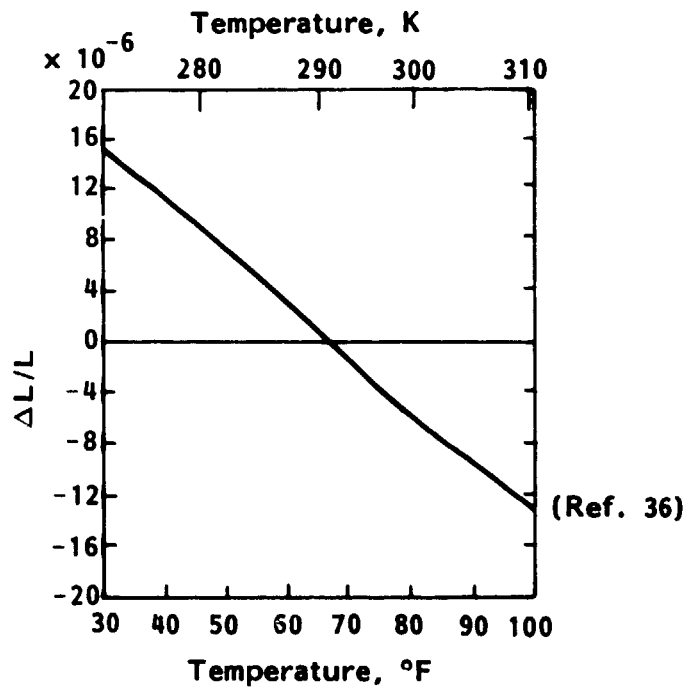

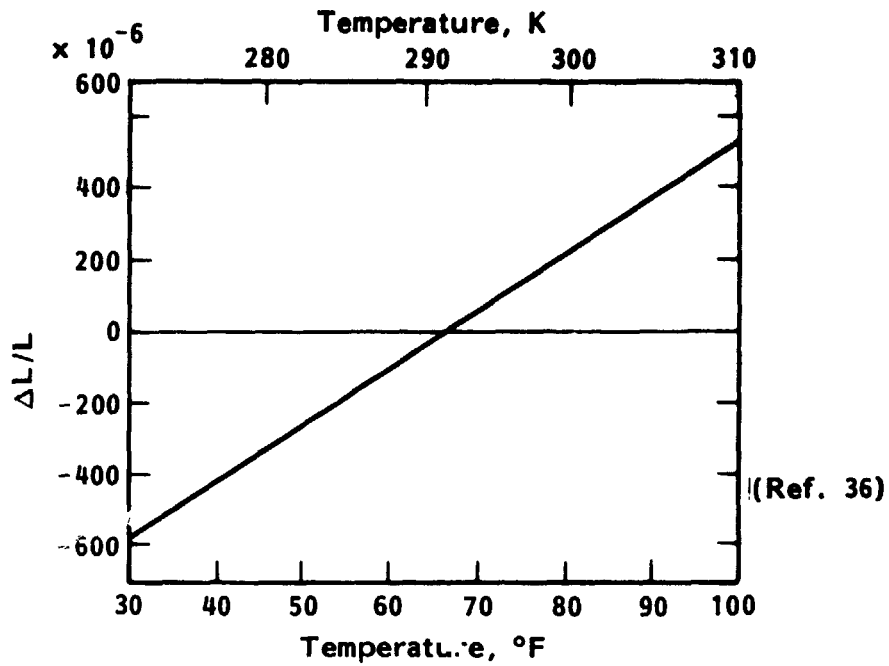Figure 30. – Thermal expansion of HMS/934 unidirecticnal tape (0° fiber direction).

45

Figure 31. — Thermal expansion of HMS/934 undirectional
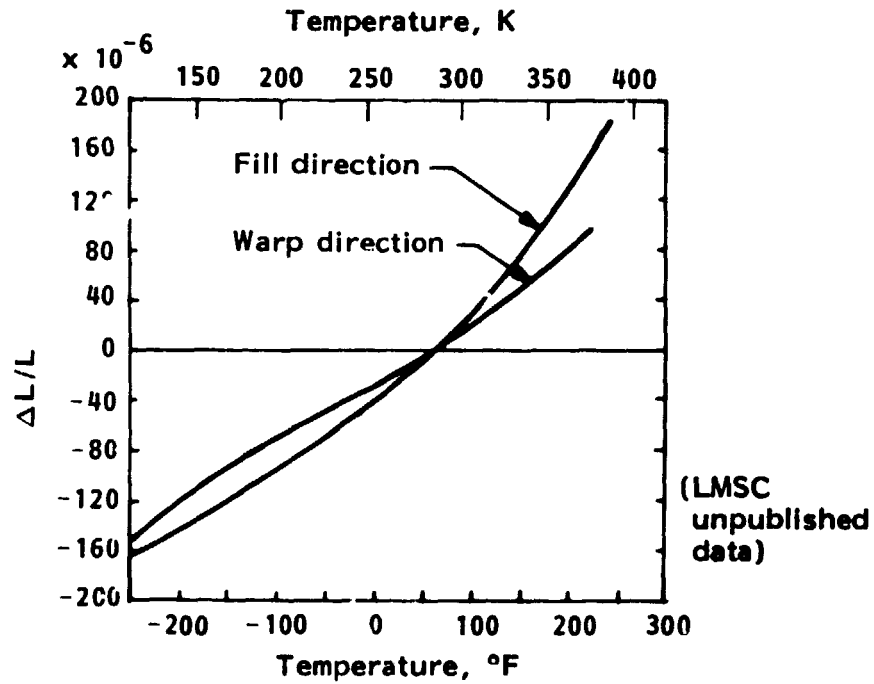tape (90° fiber direction).

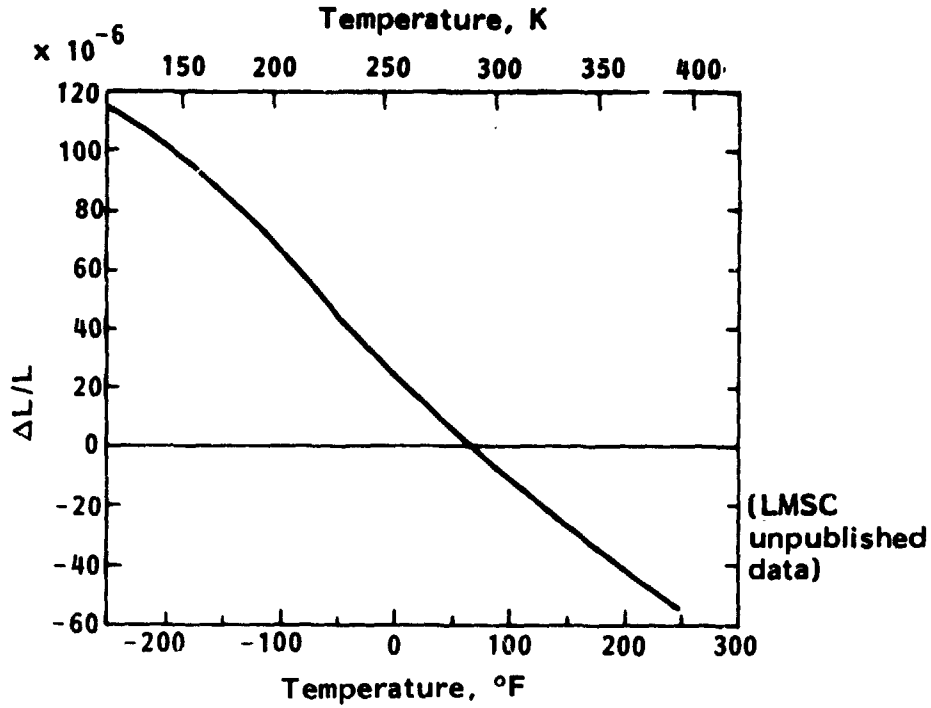Figure 32. — Thermal expansion of HMS/E788 fabric.

46

Figure 33. — Thermal expansion of unidirectional Thornel-50 (Pan)/F263 tape (0° fiber direction).
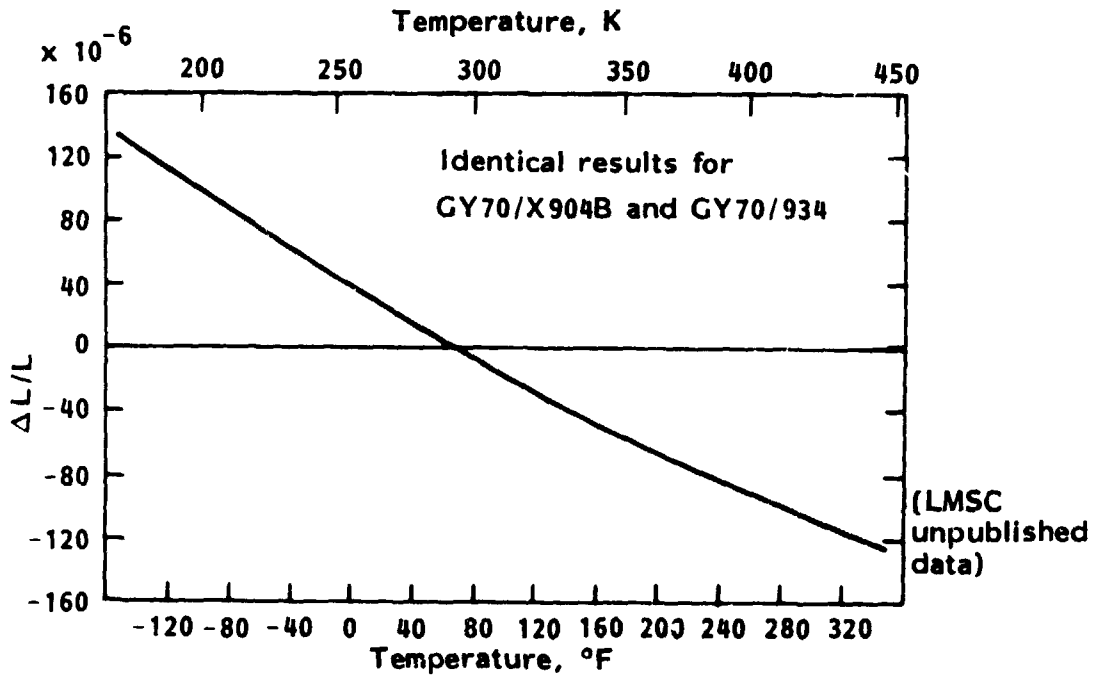

Figure 34. — Thermal expansion of GY70/epoxy unidirectional tape (0° fiber direction).
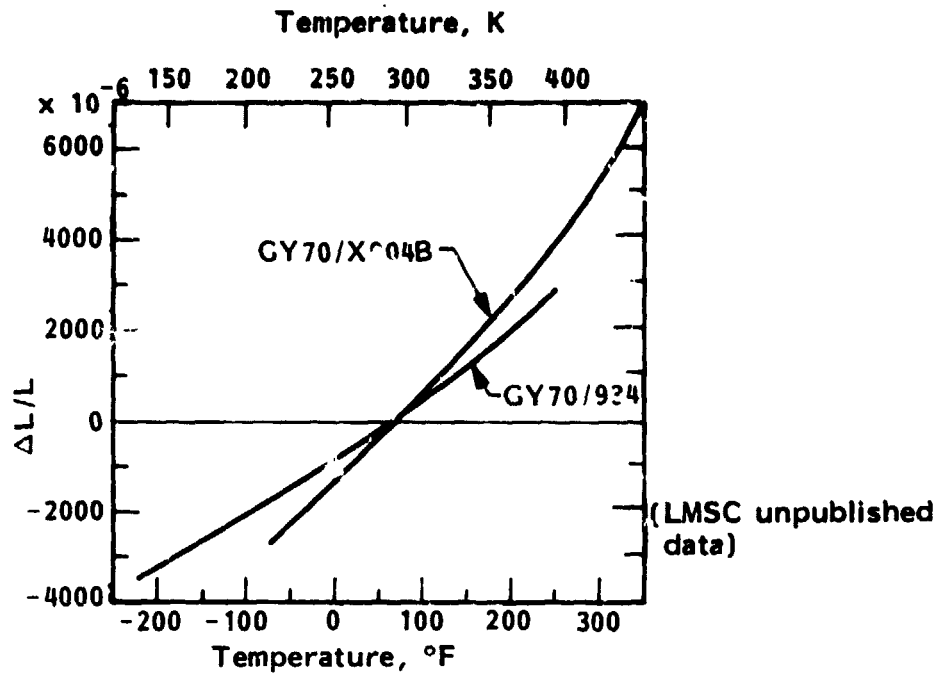
Figure 35. – Thermal expansion of GY70/X904B and GY70/934
unidirectional tape (90° fiber direction).
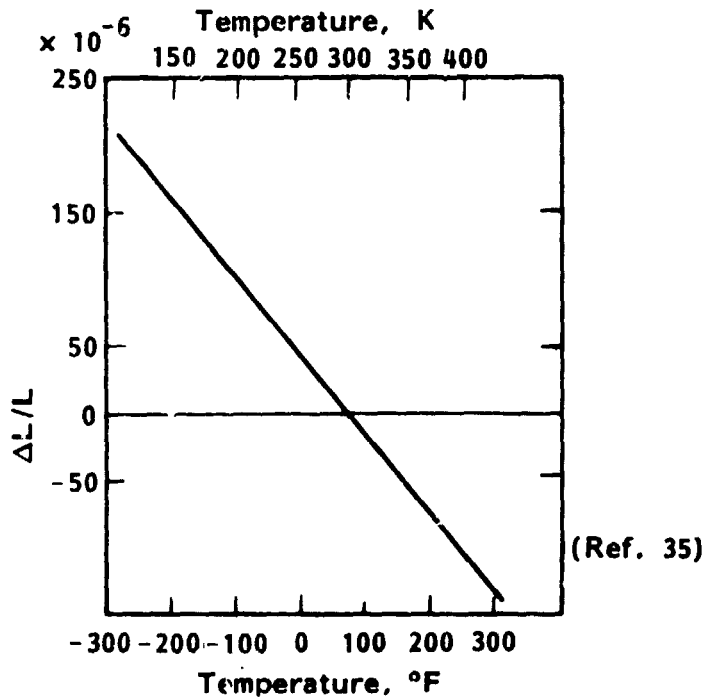

Figure 36. – Longitudinal (0°) thermal expansion
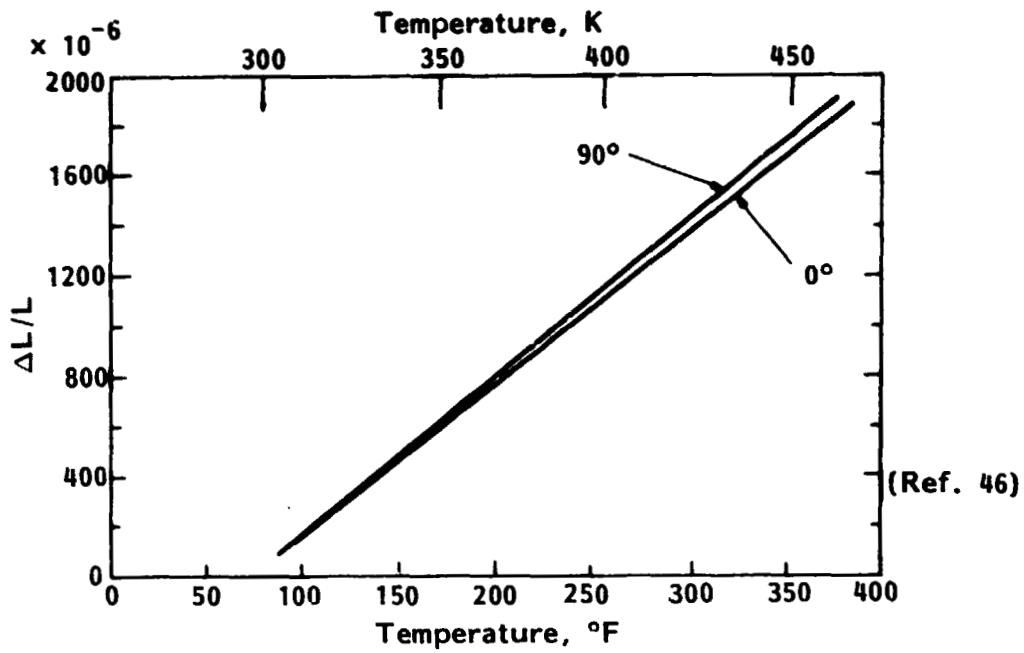of P75S/934, graphite/epoxy.

48

Figure 37. – Thermal expansion of glass/epoxy tooling material (181 cloth laminate).
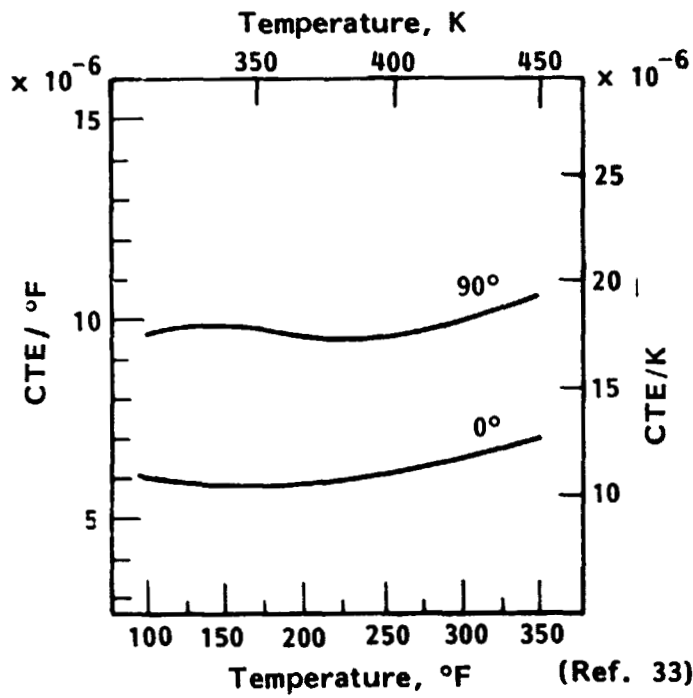

Figure 38. – Thermal expansion of 104 glass scrim cloth.

REFERENCES

1. Achievable Flatness in Large Microwave Power Antenna Study. NASA-CR-151831, General Dynamics Corporation, August 1978.

2. Kural, M.: Sensitivity Analysis for CTE of a Graphite Epoxy Laminate. LMSC S/I-1791, September 20, 1978.

3. Schapery, R. A.: Thermal Expansion Coefficients of Composite Materials Based on Energy Principles. J. Comp. Materials, vol. 2, pp. 380, 1968.

4. Ashton, J. E.; Halpin, J. C.; and Petit, P. H.: Primer on Composite Materials: Analysis. Progress in Materials Science Series, vol. III, Technomic Publishing Co., Inc., 1969.

5. Geiler, D. E.: Analysis, Test, and Comparison of Composite Material Laminates Configured for Low Thermal Expansion. Proceedings of 28th Annual Technical Conference, Reinforced Plastics/Composites Institute, The Society of the Plastics Industry, Inc., 1973.

6. Fahny, A. A.; and Cunnington, T. G.: Investigation of Thermal Fatigue in Fiber Composite Materials. NASA-CR-2641, July 1976.

7. Jones, R. M.: Mechanics of Composite Materials. Scripta Book Company, 1975.

8. Mauri, R. E.; Crossman, F. W.; and Warren, W. J.: Assessment of Moisture Altered Dimensional Stability of Structural Composites. Proceedings of 23rd National SAMPE Symposium, May 1978.

9. Crossman, F. W.; and Flaggs, D. L.: Dimensional Stability of Composite Laminate During Environmental Exposure. Proceedings of the 24th National SAMPE Symposium, May 1979.

10. Dong, S. B.; Pister, K. S.; and Taylor, R. L.: On the Theory of Laminated Anisotropic Shells and Plates. J. Aero, Sci., 28, 969, 1962.

11. Reissner, E.; and Stavsky, Y.: Bending and Stretching of Certain Types of Heterogeneous Aeolotropic Elastic Plates. J. Applied Mechanics, 28, 402, 1961.

12. Tsai, S. W.: Introduction to Mechanics of Composite Materials, Part II – Theoretical Aspects. AFML-TR-66-149, Air Force Materials Laboratory, Wright-Patterson AFB, 1966.

13. Tsai, S. W.; and Pagano, N. J.: Invariant Properties of Composite Materials. AFML-TR-67-349, March 1968.

50

14. Halpin, J. C.; and Pagano, N. J.: Consequences of Environmentally Induced Dilatation in Solids. AFML-TR-68-375, December 1969.

15. Chamis, C. C.; and Sendecky, G. P.: Critique on Theories Predicting Thermoelastic Properties of Fibrous Composites. J. Comp. Material, 2, 332, 1968.

16. Ishikawa, T.: Thermal Expansion Coefficients of Unidirectional Composites. J. Comp. Material, 12, 153, 1978.

17. Bradstreet, S. W.; and Davis, L. W.: Prediction of Thermal Expansion in Simple Solids and its Control in Structural Composites. AIP Conf. Proc. No. 3, 1971.

18. Wakashima, K.; Otsuka, M.; and Umekawa, S.: Thermal Expansion of Heterogeneous Solids Containing Aligned Ellipsoidal Inclusions. J. Comp. Material, 8, 391, 1974.

19. Rosen, B. W.; and Hashin, Z.: Effective Thermal Expansion Coefficients of Composite Materials. Int. J. Eng. Sci., vol. 8, pp. 157, Pergamon Press, 1970.

20. Wang, A.S.D.; Pipes, R. B.; and Ahmadi, A.: Thermoelastic Expansion of Graphite/Epoxy Unidirectional and Angle Ply Composites. ASTM STP 580, 1975.

21. Design, Fabrication and Test of a Graphite/Epoxy Metering Shell (GEMS). NASA-CR-143870. Final Report (June 1973 – April 1975). April 19, 1975.

22. Arnts, Jr., G. W.: Structural Design of Space Telescope. Transportation Engineering Journal of ASCE, pp. 363, May 1976.

23. Nelson, P. T.: Strut with Infinitely Adjustable Thermal Expansivity and Length. NASA TM-X-3274, August 1975. (Ninth Aerospace Mechanisms Symposium, October 17-18, 1974.)

24. Nelson, P. T.; and Krim, M. H.: A Thermally Inert Cylindrical Truss Concept. NASA TM-X-3377, pp. 275. Part I, 3rd Conference on Fibrous Composites in Flight Vehicle Design, April 1976.

25. Wolff, E. G.: Measurement Techniques for Low Expansion Materials. Materials and Processes — In Service Performance, vol. 9, National Sampe Technical Conference Series, October 1977.

26. ASTM Method of Test, E228 – 71, for Linear Thermal Expansion of Rigid Solids with a Vitreous Silica Dilatometer. 1971 Book of ASTM Standards, Part 31.

27. Freeman, W. T.; and Campbell, M. D.: Thermal Expansion Characteristics of Graphite Reinforced Composite Materials, Testing and Design. ASTM STP 497, ASTM, pp. 121-142, 1972.

28. Fitzer, E.: Thermophysical Properties of Materials. North Atlantic Treaty Organization (AGARD-606), March 1977.

29. Taylor, R. E.; and Denman, G. L., eds: AIP Conference Proceedings No. 17, Thermal Expansion – 1973 (Lake of the Ozarks). American Institute of Physics, 1974.

30. Kingery, W. D.: Property Measurements at High Temperature. John Wiley & Sons, Inc., New York; Chapman and Hall, Limited, London, 1959.

31. Hollenberg, G. W.; and Sharpe, W. N.: Measurement of Thermal Expansion at High Temperatures by Laser Interferometry of Two Fibers. Rev. Sci Instrum., vol. 47, no. 12, December 1976.

32. Standard Method of Test for Coefficient of Linear Thermal Expansion of Plastics. ASTM Method of Test, D-696, 1980.

33. Advanced Composites Design Guide. Air Force Flight Dynamics Laboratory, vol. IV, January 1977.

34. Dow, N. F.; and Rosen, B. W.: Zero Thermal Expansion Composites of High Strength and Stiffness. NASA-CR-1324, General Electric Company, May 1969.

35. Development of Advanced Composites Equipment Support Module. Contract F33615-79-C-3202, Interim Technical Report No. 3, SSD 80-0044, Rockwell, International, February 1980.

36. Thermal Expansion Measurements of Advanced Composite Materials. LMSC-D492926, 62-61/S/R-156, Lockheed Missiles & Space Company, Inc., September 1975.

37. Advanced Composite Material Characterization Tests – T300/5209. Report No. LR28222, Lockheed-California Company, December 22, 1977.

38. Development of Engineering Data on the Mechanical and Physical Properties of Advanced Composite Materials. AFML-TR-72-205, Part 1, September 1972.

52

39. Pinhero, M. de F. F.; and Rosenberg, H. M.: A Carbon-Fiber Reinforced Composites with Zero Expansion in the Low Temperature Range. IPC Business Press, pp. 50, 1978.

40. Advanced Composite Design Data for Spacecraft Structural Applications. Report No. ASD-AFS-78-006, Second Quarterly Interim Technical Report (1 July 1978 to 1 October 1978), General Dynamics, Convair Division, Contract No. F33615-77-C-5279.

41. Development of Engineering Data on Advanced Composite Materials. AMFL-TR-77-151 Final Technical Report (1 March 1975 to 30 June 1977), University of Dayton Research Inst., Contract No. F33615-75-C-5085.

42. Neubert, H. D.: Thermally Inert Composite Hardware Applications for Spacecraft. SAMPE Journal, pp. 6-14, May/June 1978.

43. Hofer, K. E.: Development of Engineering Data on the Mechanical and Physical Properties of Advanced Composite Materials. AFML-TR-74-266, February 1978.

44. Development of Engineering Data for Advanced Composite Materials. AFML-TR-70-108, vol. 1, October 1972.

45. Mechanical and Thermal Test Results for Graphite Epoxy Systems (Unidirectional HMS/CE-339 and Woven HMF-330C/CE-339). LMSC-D579809, Lockheed Missiles & Space Co., Inc., December 1975.

46. Advanced Composite Applications for Spacecraft and Missiles. GDC-CHB70-001, Progress Report No. 4, January 1971 – June 1971. (AFML-TR-71-186, vol. 1, March 1972.